

Polymer Analysis: Molar Mass Determination

3.1 Definition of Molar Mass Parameters – 40

3.2 Absolute Methods – 44

3.2.1 End Group Analysis – 44

3.2.2 Colligative Properties – 45

3.2.3 Membrane Osmometry – 48

3.2.4 Vapor Pressure Osmometry – 50

3.2.5 Ultracentrifuge – 52

3.2.6 Light Scattering – 58

3.2.7 MALDI-TOF-MS – 77

3.3 Relative Methods – 80

3.3.1 Viscometry – 82

3.3.2 Size Exclusion Chromatography (SEC) – 86

References – 91

A key parameter for macromolecular substances is their molar mass or degree of polymerization. This chapter focuses on the question of how to describe mathematically and measure experimentally the molar mass of polymers and their molar mass distribution. A number of the methods presented have been developed exclusively for this purpose and are thus not commonly found in laboratories unconcerned with polymer chemistry. In addition to the molar mass, we discussed in ► Chap. 2 that the polymer size (e.g., of the entangled polymer coil in the melt or in solution) depends on the degree of polymerization. Therefore some methods addressing this question are also presented.

Experimental methods for defining molar mass can be divided into two basic categories: those referred to as “absolute methods,” the results of which can be directly converted to a molar mass, and a second group of methods, the “relative methods,” from which the results need to be calibrated with samples of known molar mass to infer the molar mass of the unknown sample.

In what follows, the theory on which the methods are based is briefly introduced before the most important absolute and relative methods are discussed in ► Sects. 3.2 and 3.3.

3.1 Definition of Molar Mass Parameters

Small molecules can usually be characterized by a particular molar mass. All the molecules of a sample of such a compound have the same molar mass. Anomalies are only created by different isotopes, for example, in chlorinated compounds, and are normally not considered further. The average value of the isotopic distribution is defined as the molar mass. This simple method cannot be used for polymers. As described in Chap. 8 and subsequent chapters, most polymerization methods result in a mixture of molecules with different chain lengths, each chain, in some cases, being made up of a very large variety of monomer units. The molar mass of a polymer can also be defined by an average value, but for a broad distribution the average can be calculated in several different ways. This can be demonstrated by looking at a simple example.

Example

Assume that a polymer sample contains three separate molecules, two of which have a molar mass of 10,000 g/mol and the third has a molar mass of 20,000 g/mol. If the average molar mass of this sample is required, the “intuitive” answer is 13,333 g/mol. Mathematically, the weights of the individual molecules are weighted according to their number and added together, and the sum is divided by the total number of molecules. Thus,

$$\begin{aligned} \text{Mean} &= \frac{2 \cdot 10 \text{ kg/mol} + 1 \cdot 20 \text{ kg/mol}}{2 + 1} \\ &= \frac{2}{3} \cdot 10 \text{ kg/mol} + \frac{1}{3} \cdot 20 \text{ kg/mol} \\ &\approx 13.3 \text{ kg/mol} \end{aligned} \quad (3.1)$$

Generally, the number or amount n_i of the molecules that have a molar mass M_i is multiplied with this molar mass M_i , and the sum of these products divided by the total number of molecules or the total amount of the sample. Alternatively, the product of the molar

mass M_i and the mole fraction ($x_i = n_i / \sum n_i$) can be used. The “average” calculated from this formula is called the “number average” M_n :

$$M_n = \frac{\sum_i n_i \cdot M_i}{\sum_i n_i} = \frac{\sum_i m_i}{\sum_i n_i} = \sum_i \left(\frac{n_i}{\sum_i n_i} \cdot M_i \right) = \sum_i x_i \cdot M_i \quad (3.2)$$

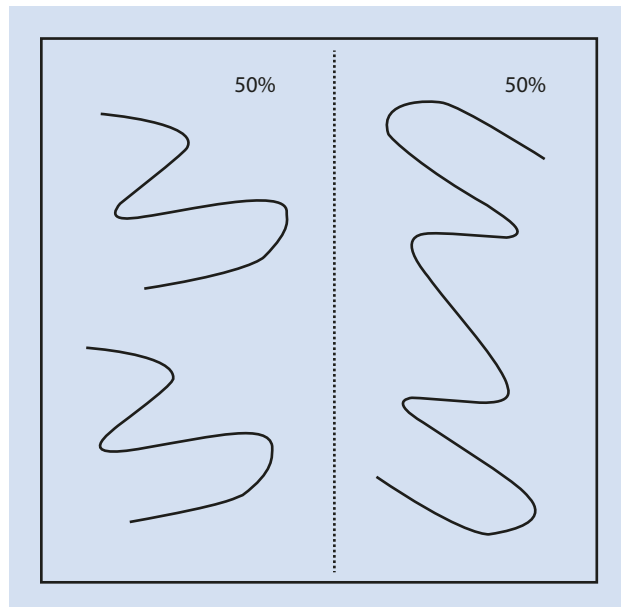
where m_i is the total mass of all molecules with a molar mass M_i . This is given by the product of the number of molecules with a molar mass M_i , n_i , and their individual molar mass M_i .

In the following the index i is omitted from the summation (sigma) characters; all the sums are valid over all i .

In the preceding equations, all molecules were weighted according to their *number* and these products used for building an average (thus the term “number average”, M_n). This average is the one often used in daily life and has thus become intuitive. However, other averages are just as mathematically valid and indeed provide different information about the distribution of the individual items in the sample. To illustrate this, the sample is not considered in terms of the number of molecules in the sample—as chemists mostly do—but in terms of the mass of each molecule type (■ Fig. 3.1).

From a material scientist’s point of view, the situation for the sample shown in ■ Fig. 3.1 is that half of the material consists of polymers with a molar mass of 10,000 g/mol and the other half of polymers with a molar mass of 20,000 g/mol. From this perspective it makes sense to assume a mean value of $((10+20)/2) = 15,000$ g/mol. In analogy to the formula for the number average molar mass, this so-called *weight average* molar mass M_w can be calculated as follows.

■ Fig. 3.1 Sketch showing a polymer sample emphasizing the weight fractions (for an explanation see text)



The mass of all molecules with the molar mass M_i is given by the product of n_i and their individual mass M_i . Thus, if in (3.2) the amount of the molecules is replaced by their mass m_i or the mole fraction with the mass fraction w_i :

$$M_w = \frac{\sum m_i \cdot M_i}{\sum m_i} = \sum \left(\frac{m_i}{\sum m_i} \cdot M_i \right) = \sum w_i \cdot M_i \quad (3.3)$$

where w_i is the mass fraction of the molecules with a molar mass M_i , that is, their mass divided by the total mass of the sample.

As the mass of the molecules in the sample is given by the sum of the products of the amount of substance and molar mass, one can also write

$$M_w = \frac{\sum (n_i \cdot M_i) \cdot M_i}{\sum (n_i \cdot M_i)} = \frac{\sum n_i \cdot M_i^2}{\sum n_i \cdot M_i} \quad (3.4)$$

In analogy with the above, it is possible to obtain further averages, although the derivations are not as straightforward as those for the number and weight averages. The centrifugal average M_z is especially important and is defined by the following equation:

$$M_z = \frac{\sum n_i \cdot M_i^3}{\sum n_i \cdot M_i^2} = \frac{\sum w_i \cdot M_i^2}{\sum w_i \cdot M_i} \quad (3.5)$$

The term “centrifugal average” is derived from this average, being that determined from ultracentrifuge measurements (► Sect. 3.2.5).

By definition, the mean molar mass increases in the following order:

$$M_n \leq M_w \leq M_z \quad (3.6)$$

From this it follows that these averages only take on the same value if *all* of the molecules of a sample are of exactly the same length and composition. Such samples, homogeneous with respect to their molar mass, are referred to as *monodisperse*. In practice, this is the exception, one rare example being DNA. In non-monodisperse or so-called *polydisperse* samples, the quotient of weight and number averages is a measurement of the breadth of the molar mass distribution. This quotient is referred to as the polydispersity index *PDI*:

$$PDI = \frac{M_w}{M_n} \quad (3.7)$$

A monodisperse sample has $PDI=1$. The larger the *PDI*, the broader the molar mass distribution.

Another measure, the *molecular non-uniformity* U of a sample, can be defined as in (3.8) (► Sect. 9.4.3):

$$U = PDI - 1 = \frac{M_w}{M_n} - 1 \quad (3.8)$$

Alternatively, the breadth of a molar mass distribution can also be characterized by its variance σ^2 :

$$\sigma^2 = \frac{\sum n_i (M_i - M_n)^2}{\sum n_i} \quad (3.9)$$

or its absolute standard deviation $\sqrt{\sigma^2}$.

A relative standard deviation, normalized with respect to M_n , $\sqrt{\sigma^2} / M_n$, can also be defined:

$$\frac{\sqrt{\sigma^2}}{M_n} = \sqrt{U} \quad (3.10)$$

From these definitions it can be calculated that even for a polymer with a narrow molar mass distribution, that is, $PDI = 1.04$, the relative standard deviation is still substantial: 20 %.¹

The number of repeating units in a polymer chain is referred to as the *degree of polymerization* P . If the end groups are neglected, P equals the quotient of the molar mass of the polymer chain and the molar mass of the repeating unit M_{RU} . As with the molar mass, the degree of polymerization of a polymer sample usually has the same (identical) distribution. Thus, the number and weight average degrees of polymerization can be defined as in (3.11) and (3.12), respectively:

$$P_n = \frac{M_n}{M_{RU}} \quad (3.11)$$

$$P_w = \frac{M_w}{M_{RU}} \quad (3.12)$$

1 The relation $\sqrt{\sigma^2} / M_n = \sqrt{U}$ is a result of the following calculation:

$$\begin{aligned} \frac{1}{M_n^2} \sigma^2 &= \frac{1}{M_n^2} \frac{\sum n_i (M_i - M_n)^2}{\sum n_i} = \frac{1}{M_n^2} \frac{\sum n_i (M_i^2 - 2M_i M_n + M_n^2)}{\sum n_i} \\ &= \frac{1}{M_n^2} \left[\frac{\sum n_i M_i^2}{\sum n_i} - 2M_n \frac{\sum n_i M_i}{\sum n_i} + M_n^2 \frac{\sum n_i}{\sum n_i} \right] \\ &= \frac{1}{M_n^2} \left[\frac{\sum n_i M_i^2}{\sum n_i} - M_n^2 \right] = \frac{1}{M_n^2} \frac{\sum n_i M_i^2}{\sum n_i} - 1 = \left(\frac{\sum n_i M_i^2}{\sum n_i M_i} \right) \frac{\sum n_i M_i}{\sum n_i} - 1 \\ &= \frac{\sum n_i}{\sum n_i M_i} \frac{\sum n_i M_i^2}{\sum n_i M_i} - 1 = \frac{M_w}{M_n} - 1 = U \end{aligned}$$

3.2 Absolute Methods

3.2.1 End Group Analysis

If polymers always include a certain number ξ of end groups, regardless of their size, and if they do not contain rings or have branched chains, the molar mass of a polymer can be calculated by quantitatively determining its end groups. The basic idea is to analyze the amount of substance making up the end groups in a certain mass of polymer. The quantitative analysis of the end groups can be carried out chemically or spectroscopically, depending on whether the end groups have a well-defined spectroscopic characteristic or are susceptible to a selective chemical reaction. A typical example of end group analysis using a chemical method is a titration. Thus, a known mass m_2 of a polymer is titrated with the measured amount of reagent n_R necessary to complete the reaction with all the end groups. In this case, $m_2 = \sum n_i M_i$ and $n_R / \xi = \sum n_i$, and from the quotient of these two values the number average molar mass of the polymer can be calculated:

$$M_n = \frac{m_2}{n_R / \xi} \quad (3.13)$$

Example

In the end group analysis of a polyester with exactly one acid group per chain, 0.7 mL of a KOH solution with a concentration of 0.1 mol/L are consumed for the titration of $m_2 = 1$ g of polymer. From (3.13) the number average molar mass of the polyester is

$$M_n = \frac{m_2 \cdot \xi}{n_R} = \frac{1 \text{ g} \cdot 1}{0.7 \cdot 10^{-3} \text{ L} \cdot 0.1 \text{ mol/L}} \approx 14,300 \text{ g/mol} \quad (3.14)$$

With increasing molar mass, this method becomes increasingly inaccurate because of the concurrent decreasing concentration of the end groups so that simple titration methods can only be used for end group analysis of molar mass up to a maximum of ca. 20,000 g/mol. Spectroscopic methods such as UV-, IR-, or ^1H -NMR-measurements are also frequently employed for the quantitative determination of the end groups and for the definition of the number average molar mass. ^{14}C - or fluorescence labeling of the end groups leads to increased sensitivity and thus to an increased measurement range for the method.

End group analysis is sometimes referred to as the *functional equivalence method*. An important precondition for the applicability of this method is an exact knowledge of the well-defined end groups.

For the special case where the molar mass is determined from an analysis of the end groups by ^1H -NMR, the weight of the polymer sample and that of the end groups are not required. In this case, the intensity of the ^1H -NMR-signals resulting from the end group are proportional to the amount of substance of the corresponding protons and these signals can be compared with those identified as resulting exclusively from the repeating unit of the chain. If the number of protons of the end group signal is given by ζ_E and the number of protons in each repeating unit by ζ_{RU} , from the corresponding intensities, I_E and I_{RU} respectively, the number average degree of polymerization is given by

$$P_n = \frac{I_{RU} / \zeta_{RU}}{I_E / \zeta_E} \quad (3.15)$$

It is worth mentioning MALDI-TOF-mass spectrometry as an additional method and because this is now widely used for polymer analyses it is discussed separately in Sect. 3.2.7.

3.2.2 Colligative Properties

If a substance is dissolved in a solvent, the chemical potential of the solvent decreases. This leads to changes in, for example, the vapor pressure, the freezing and boiling points, and the osmotic pressure of the solvent. These properties are called the colligative properties of the solution (from the Latin *colligatus* meaning *bound together*.) In a highly diluted state, changes in the colligative properties are approximately proportional to the volume fraction or the concentration of the solute. If such a dilute solution is separated from pure solvent by a membrane through which the solvent but not the solute can pass, an equilibrium can only be established by changing another thermodynamic parameter, such as the temperature or pressure, of either the solution or the pure solvent.

Such a difference allows the mole fraction of the solute and, if the weight of the solute is known, its molar mass to be determined. Changes in the colligative properties of a solution are proportional to the number of dissolved particles per volume, not their size nor, provided there is no chemical reaction between the solute and the solvent, their chemistry. Thus, the molar mass determined from the measurement of colligative properties is the number average molar mass M_n .

Boiling Point Elevation and Freezing Point Depression

If a non-volatile substance which isn't incorporated into the solvent's crystal structure when the latter freezes is dissolved in a solvent, the decrease of the chemical potential of the solvent causes the phase diagram boundaries between the liquid and the gas phase and that between the solid and the liquid phase to shift in such a way that the liquid area increases. Thus, at any pressure, the liquid-gas boundary moves to higher temperatures and the liquid-solid boundary moves to lower temperatures (■ Fig. 3.2). At a constant temperature the vapor pressure decreases, whereas at constant pressure the boiling temperature is elevated to a temperature T_b and the melting temperature is lowered to a temperature T_f .

The solution boils when the chemical potential of the solvent in the solution is the same as that of the chemical potential of the solvent in the gas phase:

$$\mu_1(\text{gas}) = \mu_1^{\text{pure}}(\text{fl}) + RT_b \cdot \ln x_1 \quad (3.16)$$

Here and in the following, $\mu_1^{\text{pure}}(\text{fl})$ is the chemical potential of the pure liquid and the subscript 1 indicates the solvent. We explicitly presume that the solute (hereafter denoted with the index 2) does not evaporate and therefore the solvent vapor is present in pure form. Because the sum of the mole fraction of the solvent and that of the solute is 1, $x_1 = 1 - x_2$, so that

$$\ln(1-x_2) = \frac{\mu_1(\text{gas}) - \mu_1^{\text{pure}}(\text{fl})}{RT_b} = \frac{\Delta_{\text{vap}}G_m}{RT_b} \quad (3.17)$$

where $\Delta_{\text{vap}}G_m$ is the molar free enthalpy of vaporization for the solvent. With

$$\Delta_{\text{vap}}G_m = \Delta_{\text{vap}}H_m - T_b \cdot \Delta_{\text{vap}}S_m \quad (3.18)$$

(3.17) can be rearranged to give

$$\ln(1-x_2) = \frac{\Delta_{\text{vap}}G_m}{RT_b} = \frac{\Delta_{\text{vap}}H_m}{RT_b} - \frac{\Delta_{\text{vap}}S_m}{R} \quad (3.19)$$

For the pure solvent, $x_2=0$ and the boiling temperature is T_b^{pure} . Because $\ln 1=0$, (3.19) for the pure solvent becomes

$$0 = \frac{\Delta_{\text{vap}}G_m}{RT_b^{\text{pure}}} = \frac{\Delta_{\text{vap}}H_m}{RT_b^{\text{pure}}} - \frac{\Delta_{\text{vap}}S_m}{R} \quad (3.20)$$

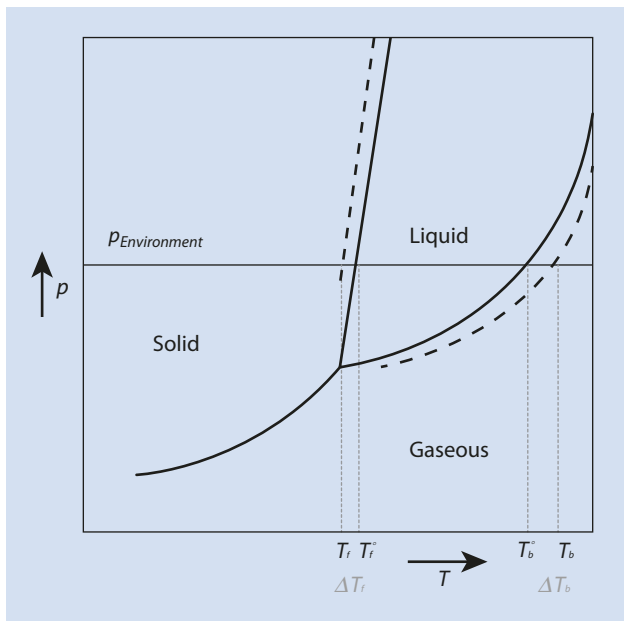
Subtracting (3.20) from (3.19) gives

$$\ln(1-x_2) = \frac{\Delta_{\text{vap}}H_m}{R} \cdot \left(\frac{1}{T_b} - \frac{1}{T_b^{\text{pure}}} \right) \quad (3.21)$$

With $x_2 \ll 1$, the approximation $\ln(1-x_2) \approx -x_2$ can be made and

$$x_2 = \frac{\Delta_{\text{vap}}H_m}{R} \cdot \left(\frac{1}{T_b^{\text{pure}}} - \frac{1}{T_b} \right) \quad (3.22)$$

Fig. 3.2 Phase diagram showing an increase of the boiling point (ΔT_b) and a decrease of the freezing point (ΔT_f) as the result of adding a solute; solution (dashed line) and pure solvent (full line)



Additionally, for dilute solutions T_b does not significantly differ from T_b^{pure} and the term in parentheses can be approximated by

$$\frac{1}{T_b^{pure}} - \frac{1}{T_b} = \frac{T_b - T_b^{pure}}{T_b^{pure} \cdot T_b} \approx \frac{\Delta T_b}{T_b^{pure^2}} \quad (3.23)$$

Here the change in the boiling point $T_b - T_b^{pure} = \Delta T_b$ is what is measured so that it is easier to rearrange the approximate form of (3.22) to give

$$\Delta T_b = \frac{R \cdot T_b^{pure^2}}{\Delta_{vap} H_m} \cdot x_2 \quad (3.24)$$

Interpreting (3.24):

- The boiling point increases because the enthalpy of vaporization is positive
- The increase (for solutions of non-volatile solutes) is directly proportional to the mole fraction of the solute
- The increase is greater, the higher the boiling temperature and the lower the enthalpy of vaporization

Using this principle, the molar mass of the solute can be determined. To this end, the mole fraction of the solute in (3.24) by the respective amounts of the components n_i is

$$x_2 = \frac{n_2}{n_1 + n_2} \approx \frac{n_2}{n_1}, \quad \text{because } n_2 \ll n_1 \quad (3.25)$$

With the molar mass of the solvent and solute, M_1 and M_2 , the total mass m and the approximation $n_1 \approx m / M_1$, it follows that

$$\Delta T_b = \frac{R \cdot T_b^{pure^2} M_1}{\Delta_{vap} H_m} \cdot \frac{n_2}{m} \equiv K_{bp} \cdot \frac{n_2}{m} \quad (3.26)$$

Here, n_2/m is the number of moles of the solute in the solution and is also referred to as the *molality* of the solution. K_{bp} is the *ebullioscopic constant* for the solvent and exclusively dependent on the properties of the solvent. K_{bp} can be seen as an empirical constant, a characteristic of a solvent, and is often known. If this is the case, by measuring the change in the boiling point for different concentrations of solute the molar mass of the solute can be determined. If a weighed amount of polymer m_2 is the solute, the molar mass measured in this way is number average M_n :

$$M_n = K_{bp} \cdot \frac{m_2}{m} \cdot \frac{1}{\Delta T_b} \quad (3.27)$$

The freezing point depression can be treated in analogy to the boiling point elevation. In this case a solid solvent (1) is considered in equilibrium with the liquid solvent with the solute (2). Mentioned above, it is assumed that the solute is not included in the crystal structure of the solid solvent.

At equilibrium:

$$\mu_1(\text{solid}) = \mu_1^{\text{pure}}(\text{fl}) + RT \cdot \ln x_1 \quad (3.28)$$

By making use of the identical argumentation as for the boiling point elevation, one obtains

$$\Delta T_f = T_f^{\text{pure}} - T_f = \frac{R \cdot T_f^{\text{pure}^2}}{\Delta_{\text{fus}} H_m} \cdot x_2 = \frac{R \cdot T_f^{\text{pure}^2} M_1}{\Delta_{\text{fus}} H_m} \cdot \frac{n_2}{m} \equiv K_{fp} \cdot \frac{n_2}{m} \quad (3.29)$$

The ΔT_f is defined in (3.29) inversely to the definition of ΔT_b given above and is the freezing point depression. Here, too, K_{fp} is an empirical constant specific to the solvent, which is referred to as the *cryoscopic constant* and $\Delta_{\text{fus}} H_m$ is the molar enthalpy of melting. The index “*fp*” stands for *freezing point*.

3.2.3 Membrane Osmometry

Another important method for determining the number average molar mass is osmometry, which is based on the change in the osmotic pressure of a polymer solution as compared to the pure solvent.

Osmometry is an absolute method which, in the same way as the boiling point elevation and the freezing point depression, relies on colligative properties. An osmotic pressure is created when the solution and solvent are separated by a semipermeable membrane, which ideally is only permeable for the solvent molecules, not for the solute. If that part of the apparatus which contains the solution is sealed and connected to a manometer, the solvent passes through the membrane until a pressure difference of Π is built up, which is as large as is necessary for the chemical potentials to be equal on both sides of the membrane (■ Fig. 3.3). The hydrostatic pressure is given by the height change in the manometer Δh .

In contrast to the boiling and freezing point measurements, carried out at a constant pressure, the measurement of the osmotic pressure is carried out at a constant temperature and this is important for the mathematical treatment of the results.

At equilibrium at a constant temperature, the chemical potential of the pure solvent at a pressure p is equal to the chemical potential of the solvent of a solution whose mole fraction is x_1 at a pressure $p + \Pi$:

$$\mu_1^{\text{pure}}(p) = \mu_1(x_1, p + \Pi) \quad (3.30)$$

The different terms $\mu_1(x_1, p + \Pi)$ need to be examined more closely. The free enthalpy and thus the chemical potential is a function of state. To derive $x_1 = 1 - x_2$ $p + \Pi$ from $x_1 = 1$, P one can conceptually increase the pressure and then add solute 2. Because $d\mu/dp = V_m$, it follows for the chemical potential:

$$\begin{aligned} \mu_1(x_1, p + \Pi) &= \mu_1^{\text{pure}}(p + \Pi) + RT \cdot \ln x_1 \\ &= \mu_1^{\text{pure}}(p) + RT \cdot \ln x_1 + \int_p^{p+\Pi} V_m^1 dp' \end{aligned} \quad (3.31)$$

where V_m^1 is the molar volume of the solvent and p' is an auxiliary variable for the pressure to facilitate integration. Combining (3.30) and (3.31) and rearranging gives

$$-RT \cdot \ln x_1 = \int_p^{p+\Pi} V_m^1 dp' \quad (3.32)$$

If the molar volume is constant, with

$$-RT \cdot \ln(1 - x_2) \approx RTx_2, \quad (3.33)$$

it follows that

$$RT \cdot x_2 = V_m^1 \Pi \quad (3.34)$$

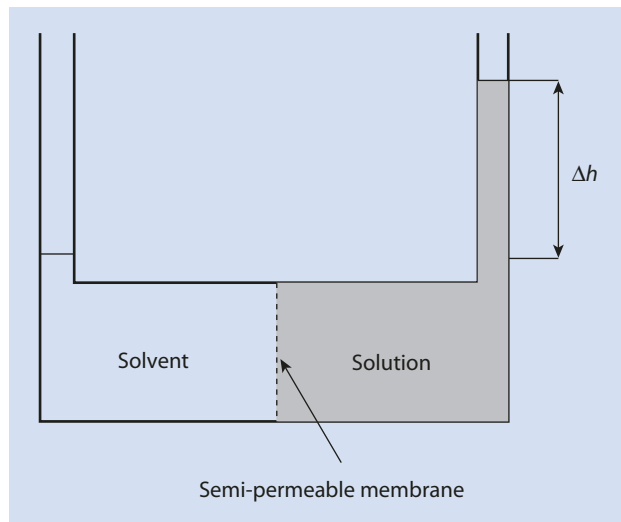
With $x_2 \approx n_2 / n_1$ (dilute solution) and $n_1 V_m^1 = V$, one obtains a variant of the van't Hoff equation:

$$\Pi V = n_2 RT \quad (3.35)$$

However, for solutions of large molecules such as polymers, deviations from this equation often arise even at low concentration. To account for such deviations, real solutions are described, e.g., by a *virial equation*. For the case in hand, this is a polynomial of the concentration. Hereby the nonlinear portions of the concentration, which according to the derivation above should not need to be accounted for, are mathematically included. In this virial equation the quotient n_2/V is expressed by the quotient of the mass concentration c_2 and the molar mass M_2 and

$$\Pi = RT \left(\frac{1}{M_2} c_2 + A_2 c_2^2 + A_3 c_2^3 + \dots \right) \quad (3.36)$$

■ Fig. 3.3 Principle of an osmometer (Pfeffer Cell)



By taking measurements at various concentrations and extrapolating the results to $c_2 = 0$, the molar mass can be obtained from

$$\lim_{c_2 \rightarrow 0} \left[\frac{\Pi}{c_2} \right] = RT \frac{1}{M_2} \quad (3.37)$$

The value obtained is the number average molar mass.

If, rather than a simple extrapolation which ignores the nonlinear terms, the results are analyzed, one obtains a measure of the non-ideality of the system.

The parameters A_2, A_3, \dots are referred to as the *virial coefficients* of the osmotic pressure. With the aid of the algebraic sign one can determine whether the solvent can be considered as “good” (positive sign) or “poor” (negative sign). With this method a relationship can be established to the experimental determination of the Flory–Huggins parameter (► Chap. 2) for dilute solutions. Thus, it holds (without proof) that:

$$A_2 = \frac{1}{M_{RU} \rho_2} (1 - \chi) \quad (3.38)$$

where M_{RU} is the molar mass of the repeating unit, ρ_2 the polymer density (or $1/\rho_2$ the specific volume of the polymer), and χ the Flory–Huggins parameter.

Thus, with membrane osmometry the osmotic pressure between a polymer solution and the pure solvent is measured. This can be accomplished by using a simple manometer or, more usually, by direct pressure measurement in a closed system.

This absolute method can be used successfully in the molar mass range of 10^4 to 10^6 g/mol. The lower limit is given by the quality of the membranes, which usually become permeable for smaller molecules. The upper limit is because of Π being proportional to x_2 (Π being inversely proportional to M_2). Thus, the effect being measured becomes smaller as the size of the molecules increases and at some point the margin of error makes reliable measurement impossible.

Example

In a membrane osmometer, the pressure differences between pure water and polyethylene oxide solutions are determined for a range of concentration. The results are then plotted as a graph of Π/c_2 vs c_2 (► Fig. 3.4) to give a straight line. Standard osmometers are often calibrated with a hydrostatic pressure difference so that the osmotic pressure

$$\Pi = \rho gh \quad (3.39)$$

where ρ is the density of the solvent, g the gravitational acceleration, and h the measured height difference.

Often only the height difference h is provided rather than the osmotic pressure Π .

Extrapolation to $c_2 = 0$ results in $\lim_{c_2 \rightarrow 0} [h/c_2] = 256 \text{ cm}^4 \text{ g}^{-1}$, from which, according to (3.37), the medium molar mass $M_n = 103 \text{ kg mol}^{-1}$ can be determined. From the gradient one can obtain $A_2 = 8.7 \cdot 10^{-4} \text{ mol cm}^3 \text{ g}^2$.

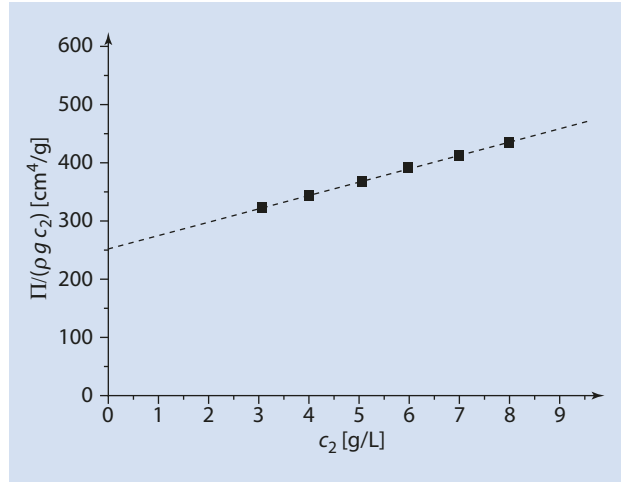
3.2.4 Vapor Pressure Osmometry

As well as membrane osmometry, vapor pressure osmometry is also an important method for determining the molar mass of polymers and this method is now discussed in more detail.

■ **Fig. 3.4** Plot of the quotient of osmotic pressure and the polymer concentration vs polymer concentration, normalized with the density of the solvent ρ and the acceleration produced by gravity g . The extrapolation to $c_2=0$ gives from the intercept with the vertical axis.

$$\lim_{c_2 \rightarrow 0} \left[\frac{\Pi}{(\rho \cdot g \cdot c_2)} \right]$$

$$= \lim_{c_2 \rightarrow 0} \left[\frac{h}{c_2} \right] = RT / M_n$$



As explained in ► Sect. 3.2.3, the vapor pressure of a solution is less than that of the pure solvent. Thus, if, in a closed chamber, both a compartment of pure solvent and one containing a solution are side by side in the same gas volume, solvent diffuses from the compartment with pure solvent (higher vapor pressure) to that of the solution (lower vapor pressure) via the gas phase. As the solvent condenses into the solution the heat of vaporization warms the solution, leading to an increase in its vapor pressure. The diffusion of solvent continues until the solution attains the same vapor pressure as the pure solvent.

Technical Setup

The floor of a tempered measuring cell (■ Fig. 3.5) is covered with solvent and equilibrated to ensure a constant vapor pressure. In the vapor chamber of the measuring cell there are two thermal sensors (e.g., thermistors). One drop of solution is applied to one of these temperature sensors, e.g., with a syringe and a drop of solvent to the other. As the vapor pressure of the drop of solution is less than the vapor pressure of the pure solvent, solvent condenses on the drop of solution. The temperature difference ΔT between the two sensors is measured.

To simplify, we can assume that this experiment corresponds to a boiling point elevation experiment—conducted with the partial pressure of the solvent—and that the experimentally determined temperature difference is evaluated (in which the boiling point temperature is to be replaced with the medium temperature of the chamber).

However, there is no real state of equilibrium inside the measuring chamber. A fixed state prevails in which material transfer and heat conduction balance each other. Moreover, the temperature of the chamber is often so distant from the boiling point that the assumption that the enthalpy of vaporization is independent of temperature is not always justifiable. These effects can be corrected, at least empirically, so that it is possible to determine reliably the medium value of the molar mass M_n of an unknown sample by calibrating the device as indicated by the manufacturer or by calibrating with a substance of known molar mass. With this method, it is also necessary to measure a concentration series and to extrapolate to c_2 (or m_2/m_1) = 0. Using a calibration constant K which has to be determined for each apparatus and each solvent:

$$M_n = K \cdot \lim_{m_2/m_1 \rightarrow 0} \left[\frac{m_2 / m_1}{T - T^0} \right]$$

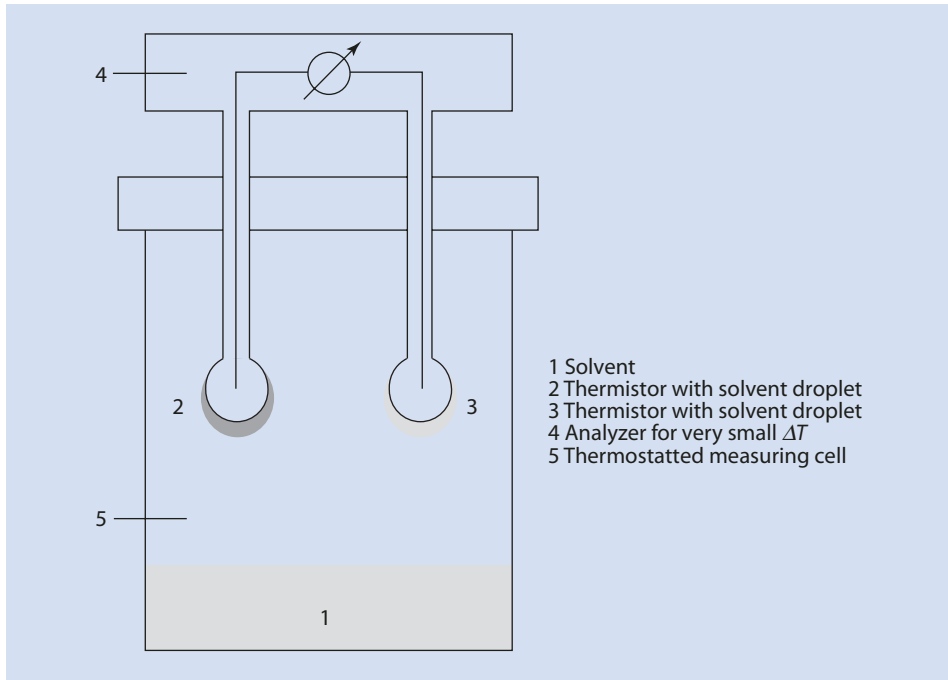


Fig. 3.5 Simplified sketch of a vapor pressure osmometer

or

$$M_n = K \cdot \lim_{m_2/m_1 \rightarrow 0} \left[\frac{m_2 / m_1}{\Delta T} \right] \quad (3.40)$$

This method also yields a number average molar mass and is less time consuming than membrane osmometry. It also requires less sample and is suitable for molar masses (M_2) less than 10^4 g/mol. Although the exact recording of absolute temperatures is difficult, it is comparatively easy to measure even minute temperature differences. Thus, vapor pressure osmometry is also suitable for polymers of high molar mass.

3.2.5 Ultracentrifuge

The ultracentrifuge (UC) is a centrifuge which rotates at very high speeds and was originally developed by Svedberg for his research on inorganic and organic colloids (Svedberg and Pedersen 1940). In a solid rotor made of light alloy, two cuvettes are embedded opposite each other, normally within a few centimeters of the axis of rotation. Their top and bottom walls consist of two parallel glass plates and the two sides are parallel to radial lines originating from the axis of rotation to prevent the development of convection patterns. In most cases a powerful optical imaging of the cuvette inside the rotor during the centrifugal process is integrated into the ultracentrifuge.

With an ultracentrifuge, essentially three types of experiment are possible, which allow conclusions about the shape, conformational changes, and size distribution of dispersed particles or dissolved macromolecules. (Maechtle and Boerger 2006).

3.2.5.1 Analysis of Sedimentation Velocity

Polymers usually have a density greater than that of smaller molecules. This can be easily explained by considering that, during polymerization, the distances between the monomer molecules determined by van der Waals forces are replaced by (shorter) covalent bonds. In the ultracentrifuge, a centrifugal force F_Z is imposed on a dispersed particle or a dissolved polymer chain and this force is dependent on the difference in density between that of the particle and that of the surrounding liquid ($\rho_2 - \rho_1$), its volume V_2 , and the rotational speed of the rotor:

$$F_Z = V_2 \cdot (\rho_2 - \rho_1) \cdot \omega^2 x \quad (3.41)$$

ω Angular velocity
 x Distance to the axis of rotation

The particle is accelerated radially outwards by the centrifugal force. The resulting movement induces a frictional force F_R acting opposite to the centrifugal force and dependent on the shape and size of the particle. It is usually also proportional to the viscosity of the surrounding fluid η and the velocity of the particle, dx/dt :

$$F_R = f \cdot \frac{dx}{dt} \quad (3.42)$$

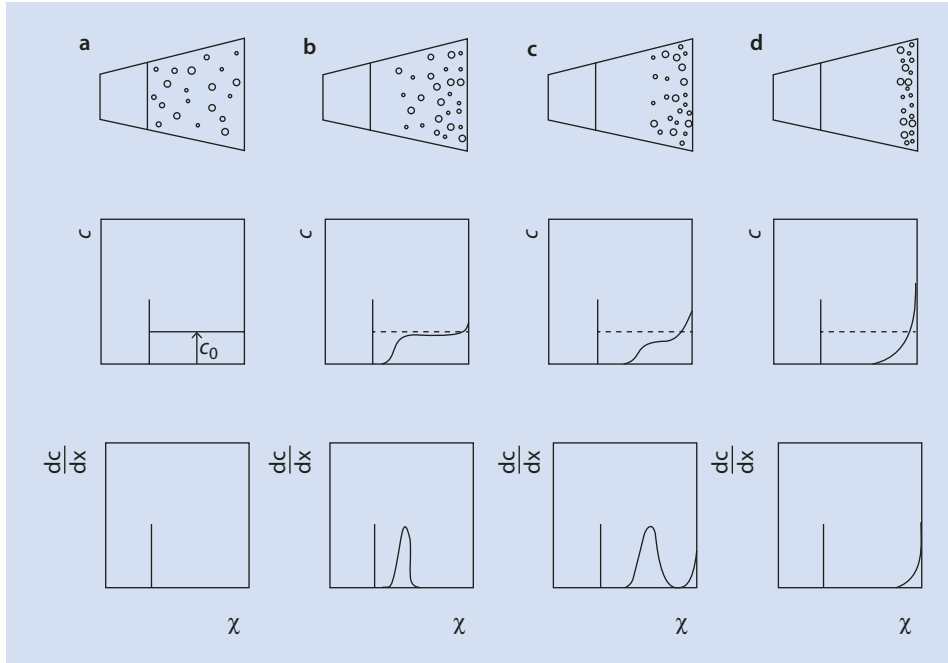
Because the shape of the particle is usually unknown, in the first instance the shape dependency is expressed by an unknown friction factor f . If the particles are spheres, the friction factor f_{sphere} is proportional to the hydrodynamic radius R_h of the particle according to Stokes' law and the viscosity of the surrounding liquid:

$$f_{sphere} = 6\pi\eta R_h \quad (3.43)$$

In the centrifuge, the particle is accelerated until the centrifugal force is balanced by the frictional force and the particle moves outwards with a constant velocity. If the particles are all the same size and shape they all move with the same velocity, and it is possible to observe a 'front' moving outwards leaving a solution free of particles or polymer molecules behind it and moving with a constant speed from the surface of the liquid towards the bottom of the cuvette (■ Fig. 3.6).

The movement of the front can be determined, e.g., by so-called *Schlieren optics* which can detect even small changes in the refractive index and thus also in the concentration (dc/dx) (■ Fig. 3.6). As soon as the particle has reached a constant velocity the forces are in equilibrium, $F_z = F_R$, so that

$$V_2 \cdot (\rho_2 - \rho_1) \cdot \omega^2 x = f \cdot \frac{dx}{dt} \quad (3.44)$$



■ Fig. 3.6 Four characteristic stages of sedimentation in the cuvette of an ultracentrifuge. (a) Uniformly distributed particles. (b) Formation of a maximum in the concentration gradient. (c) Movement of the gradient towards the base of the cuvette. (d) “Front” reaches the base of the cuvette

The ratio of the sedimentation velocity, dx/dt , and the strength of the centrifugal acceleration, ω^2x , is denoted as the sedimentation coefficient S , so that

$$S = \frac{dx/dt}{\omega^2x} = \frac{V_2 \cdot (\rho_2 - \rho_1)}{f} \quad (3.45)$$

The sedimentation coefficient has the dimensions of time (s). In honor of the pioneer of centrifugal technology, the sedimentation coefficient is usually expressed in the unit ‘Svedberg,’ 10^{-13} s (abbreviated by the symbol S). Without the knowledge of the shape, size, or density of the particle, this experiment alone does not allow an assertion extending beyond the sedimentation coefficient. In many biopolymers, this assertion suffices and the sedimentation coefficient becomes the identifier.

Notwithstanding, the diffusion coefficient D of the particle can be determined, e.g., via dynamic light scattering (► Sect. 3.2.6.2), which is linked to the friction factor f by the Einstein relation:

$$D = \frac{k_B T}{f} \quad (3.46)$$

If the density ρ_2 of the particle is also known, its volume V_2 can be derived from its molar mass M_2 and the Avogadro’s constant N_A by using

$$V_2 = \frac{m_2}{\rho_2} = \frac{M_2}{N_A \cdot \rho_2}, \quad (3.47)$$

and the molar mass can be obtained from

$$S = V_2 \cdot (\rho_2 - \rho_1) \cdot \frac{1}{f} = \frac{M_2}{N_A \rho_2} \cdot (\rho_2 - \rho_1) \cdot \frac{D}{k_B T} \quad (3.48)$$

$$M_2 = \frac{RT}{D} \cdot S \cdot \left(\frac{\rho_2}{\rho_2 - \rho_1} \right) \quad (3.49)$$

Both the sedimentation coefficient S and the diffusion coefficient D depend on the concentration so that measurements at different concentrations and the extrapolation of the measured values to $c_2 = 0$ are necessary.

For spherical particles for which the density is independent of the molar mass (e.g., inorganic particles or non-swollen polymer particles but not swollen polymer entanglements), the volume is proportional to the cube of the radius. Thus, for such spherical particles:

$$S = \frac{4}{3} \pi \cdot R_h^3 \cdot (\rho_2 - \rho_1) \cdot \frac{1}{6\pi\eta R_h} \Leftrightarrow R_h = \sqrt{\frac{9}{2} \frac{\eta S}{\rho_2 - \rho_1}} \quad (3.50)$$

According to (3.50), a radius can be calculated which a solid sphere with an equivalent sedimentation coefficient would have irrespective of the actual shape of the particle. This radius is called the *hydrodynamic radius*.

Because the molar mass M_2 of non-swollen spherical particles is obtained by multiplying the density ρ_2 with the molar volume $\left(V_2^m = \frac{4}{3} \pi R_h^3 \cdot N_A \right)$ using $M_2 = \frac{4}{3} \pi R_h^3 \cdot N_A \cdot \rho_2$, it follows for such particles that

$$M_2 = 9\sqrt{2}\pi\rho_2 N_A \left(\frac{\eta S}{\rho_2 - \rho_1} \right)^{\frac{3}{2}} \quad (3.51)$$

For particles or polymer chains having a distribution of molar mass, not all of the particles at the same distance to the rotor have the same sedimentation velocity. Thus, a sharp front which moves outwards without alteration is not observed. In a mixture of multiple, easily distinguishable sub-groups of uniform particles (e.g., protein mixtures), concentration stages can be recognized and evaluated individually. For particles or polymer chains with a broad molar mass distribution, the border between the 'particle-free' and 'particle-containing' volumes becomes more diffuse within the cuvette as the duration of the centrifugation increases. In this case, an average position for the border area can be determined and an average molar mass determined from its movement. Depending on the method used to determine the average border area, the number, weight, or centrifugal average molar mass is determined; all three average values can be determined from ultracentrifuge measurements. This is a considerable advantage of this method over the other methods discussed above.

3.2.5.2 Measurement at Thermodynamic Equilibrium

In a centrifugal force field, a particle has a potential energy E which is dependent on its distance from the rotor, its volume, and the difference between its density and that of the surrounding fluid:

$$E(x) = -\frac{1}{2}V_2 \cdot (\rho_2 - \rho_1) \cdot \omega^2 x^2 \quad (3.52)$$

If the ultracentrifuge is rotated at a velocity at which the difference between the potential energy of a particle at the bottom of the cuvette and that of a particle in the solution is of the magnitude of the product of the Boltzmann constant k_B and the temperature T , the particles are not all spun outwards but become arranged in the cuvette according to a Boltzmann distribution, so that the ratio of the concentration $c(x)$ at some distance x from the rotor axis to the concentration c_0 at a given point x_0 (e.g., the cuvette floor) is defined by

$$\frac{c(x)}{c_0} = \exp \left\{ -\frac{E(x) - E(x_0)}{2k_B T} \right\} \quad (3.53)$$

$$\frac{c(x)}{c_0} = \exp \left\{ -\frac{V_2 \cdot (\rho_2 - \rho_1) \cdot \omega^2 (x_0^2 - x^2)}{2k_B T} \right\} \quad (3.54)$$

A descriptive analogy to this dependence is the barometric formula, which describes the dependence of the density of our atmosphere on the height above sea level. However, this is with the boundary conditions that, in this case, it is not the particles in solution but rather the gas molecules in empty space which are involved and that the potential energy is, in this case, a linear and not a quadratic function of the distance from the axis (height).

From (3.54) it follows that a graph of $\ln(c(x)/c_0)$ vs $\omega^2 x^2 / (2k_B T)$ should result in a straight line with a gradient of $-V_2 \cdot (\rho_2 - \rho_1)$.

If the densities of the particle and the surrounding liquid are known, the molar mass can be calculated from

$$M_2 = \frac{[V_2 \cdot (\rho_2 - \rho_1)] \cdot N_A \rho_2}{(\rho_2 - \rho_1)} \quad (3.55)$$

If the sedimentation coefficient S is known from an analysis of the sedimentation velocity, the friction factor f (from (3.45)), the hydrodynamic radius R_h (from (3.43)), and the diffusion coefficient D (from (3.46)) can be calculated from

$$f = \frac{V_2 \cdot (\rho_2 - \rho_1)}{S} \quad (3.56)$$

$$R_h = \frac{V_2 \cdot (\rho_2 - \rho_1)}{6\pi\eta S} \quad (3.57)$$

$$D = \frac{S \cdot k_B T}{V_2 \cdot (\rho_2 - \rho_1)} \quad (3.58)$$

Compared to the analysis of the sedimentation velocity, the analysis of the sedimentation equilibrium has the advantage that, although the densities of the particle and the surrounding solution still need to be known to calculate the molar mass, the diffusion coefficient is no longer required. However, it has the disadvantage of being far more time consuming. For the measurement of sedimentation velocity, rotor speeds of up to 70,000 rpm can be selected. A single experiment suffices and one doesn't even need to wait for equilibrium to be established. Equilibrium measurements usually require a variation of rotation speeds in the region of a few thousand rpm and waiting until equilibrium is established in order to approach incrementally a sedimentation equilibrium which can be evaluated.

According to (3.54), a semi-logarithmic graph of $\ln c$ vs x^2 should result in a straight line. However, if the particles being analyzed are not of a single molar mass, the graph deviates from a straight line. In such cases it is possible to obtain number, weight, and centrifugal averages using appropriate equations. For more details, the interested reader is referred to the specialist literature. (e.g., Maechtle and Boerger 2006).

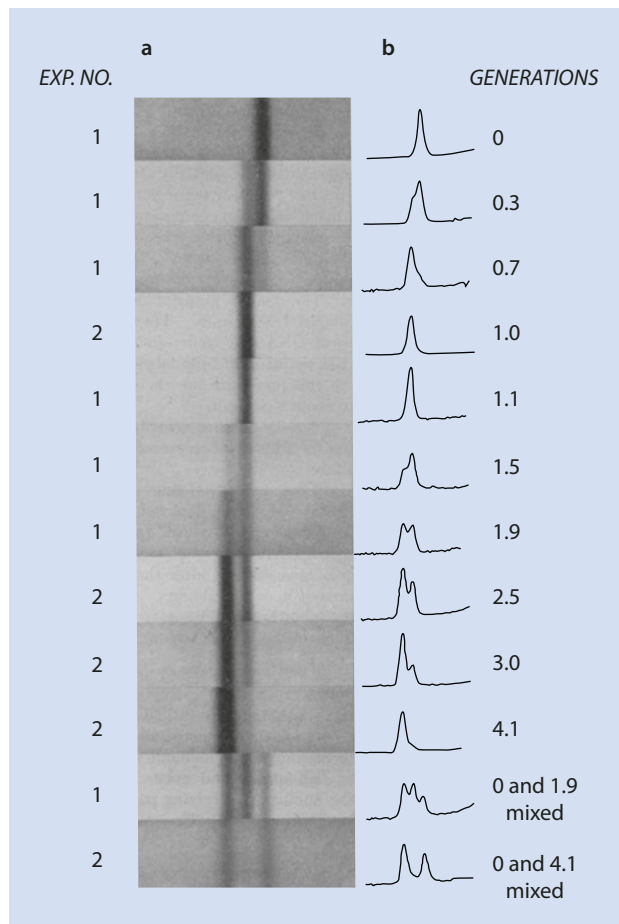
3.2.5.3 Sedimentation Equilibrium in a Density Gradient

When a liquid mixture of two low molar mass substances, e.g., an aqueous cesium chloride solution, is centrifuged in an ultracentrifuge at a high rotation speed, the substance of lower density moves to the volume facing the axis of rotation and the substance of higher density moves to the outer volume. As described in ► Sect. 3.2.5.2, a concentration gradient of the two low molar mass substances develops. If additional particles or polymer chains are present in the mixture, they move to that part of the cuvette where there is no difference between their density and that of the surrounding solution. The position of the polymers in the density gradient can be determined by analyzing the refractive index at different points with suitable imaging optics (e.g., Schlieren optics), and thus the density of particles can be determined.

As far as it is justified to assume that the two low molar mass substances used in this experiment do not influence the density of the particle or the polymer, the density determined with this method can be used to define the molar mass in conjunction with the method of sedimentation equilibrium already described (► see (3.55)).

A particularly nice example of such an experiment is shown in ■ Fig. 3.7. The photographs of the UV spectra taken during a density gradient ultracentrifuge experiment show that the genetic material in a living cell stays essentially unchanged during 'normal' metabolic processes. During cell division exactly half of the genetic material is transferred to each of the daughter cells and in each new cell the missing half is regenerated. For these experiments, microorganisms were grown in a culture medium containing nutrients enriched with the isotope ^{15}N as the sole nitrogen source. These cells were then transferred to a culture medium which only contained the lighter isotope ^{14}N as its nitrogen source and allowed to continue to multiply. At regular intervals organisms were removed, their genetic material extracted, and their density determined in an ultracentrifuge. The blackening in the bands seen in the figure is a measure of the concentration of genetic material present in the cuvette, the position of a band reflecting the density of that material (increasing from left to right). From top to bottom of the figure, the duration spent by the organisms in the new culture medium increases. It is clear that the density does not decrease with time but instead three discrete bands form: the original genetic material with 100% ^{15}N -labeling (right hand band), a middle band with 50% ^{15}N -labeling, and a third band (left hand band) which no longer contains any ^{15}N .

Fig. 3.7 UV-absorption measurements of DNA-bands of bacterial lysates after density gradient ultracentrifugation at varying times after addition of an excess of a ^{14}N -substrate to a ^{15}N -labeled cell culture. The degree of isotopic labeling of a DNA-species corresponds with the relative position of the band and lies between completely labeled and unlabeled DNA, as can be seen in the lowest photograph. Further details can be found in the literature (Meselson and Stahl 1958)



3.2.6 Light Scattering

To describe electromagnetic radiation in a dielectric it is assumed that the dielectric consists of polarizable entities stimulated and made to oscillate by an electromagnetic wave so that these in turn emit electromagnetic radiation of a frequency identical to the initial wave. The waves radially expanding from these individual sources of induced radiation interfere with each other. If the polarizable entities are all identical and equally distributed on a longitudinal scale of at least $1/20$ of the wavelength, the interference of the induced waves forms a wave which leads to constructive interference with the incident wave. Thus, stimulation by an even wave also leads to an even wave or, in other words, a ray of light shines through this medium without deflection. However, in polymer solutions the segments of the macromolecules are not homogeneously distributed within the solution (► Chap.2). In this case, components can develop from the interference of the induced radiation which deviates from the original direction of the incident wave. For a polymer solution, the polarizable entities are the repeating units of macromolecules distinguishable by their polarizability from their surroundings (the solution). On the other hand, pure solvents also display a certain scattering behavior. This is caused by local fluctuations in density and the associated inhomogeneities. In solutions of dissolved substances, additional density variations occur.

Thus, an uneven distribution of polarizable entities can originate from the molecules or particles being larger than $1/20$ of the wavelength of the incident radiation used and having a characteristic shape or from the molecules being unevenly distributed. A deflection of electromagnetic radiation by large objects of defined shape or from a regular arrangement of objects is usually referred to as *diffraction*. It is usually distinguished by sharp intensity maxima in characteristic directions. Examples of this are the opalescence of opal, moonstone, and other semi-precious stones as well as the iridescent colors of mother of pearl, insect wings, some liquid crystals, and modern effect pigments. A deflection of light by randomly arranged molecules, however, is called *scattering*. Examples of this are the blue color of the cloudless sky or the softening of sunlight by mist.

As the intensity of the scattered light depends on the shape and distribution of the particles or molecules of interest, one can draw conclusions concerning shape, distribution, and their molar mass from the angular dependence of this intensity

3.2.6.1 Static Light Scattering

In static light scattering, the time-average intensity as a function of the observation angle is measured and time-averaged information about the form and distribution of the molecules is obtained.

A polymer solution is illuminated by a light beam (■ Fig. 3.8). The intensity of the scattered light I_s is determined as a function of the observation angle θ . If a light beam of intensity I_0 is sent through a medium, it is reduced by heat development and scattering. Primary and scattered light are distinguishable by their intensity, the direction of propagation, and their state of polarization.

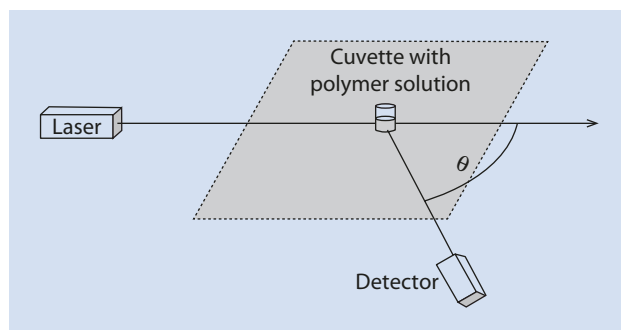
The following section is concerned with the derivation of the relevant light scattering equations. For information concerning the experimental application and the evaluation of measured data, please refer to ► Sect. "Experimental Execution and Evaluation of the Measurements".

For reasons of length and complexity of the theoretical basics of light scattering, the essential results of the derivation are again briefly summarized in ► Sect. "Experimental Execution and Evaluation of the Measurements" so that the following detailed discussion is not absolutely necessary for understanding the subsequent sections.

Theoretical Basics

To begin with, it is first assumed that the stimulation occurs by a plane wave and that this interacts with a scattering center (e.g., an isolated gas molecule or particle) which is situated in empty space. Additionally, it is assumed that the scattering centers are considerably

■ Fig. 3.8 Principle of a light scattering analyzer. Incident and observation directions cross in the cuvette and span a plane



smaller than the wavelength of the incident light so that their shape has no influence on the process and no interactions occur which could force them into preferred pattern. The scattering centers can thus be described as being randomly distributed and without short range order.

The stimulating plane wave produces an electrical field E at the site of the scattering center, which oscillates with the frequency ν :

$$E = E_0 \cdot \cos(2\pi\nu \cdot t) \quad (3.59)$$

E	Electrical field of the light-wave
E_0	Amplitude of the electrical field
ν	Frequency of the incident light
t	Time

The intensity I_0 of the incident wave, i.e., the time average of the ratio of the strength of the radiation and the irradiated area, equals

$$I_0 = c\varepsilon_0 \langle E^2 \rangle = c\varepsilon_0 E_0^2 \langle \cos^2(2\pi\nu \cdot t) \rangle = c\varepsilon_0 \frac{E_0^2}{2} \quad (3.60)$$

ε_0	Permittivity of a vacuum
c	Speed of light

The angular brackets $\langle \dots \rangle$ denote the formation of the average value over a longer time.

If the electromagnetic wave encounters a scattering center, a dipole moment μ is induced by the electrical field of the light-wave E , whose strength is proportional to its polarizability α :

$$\mu = \alpha \cdot E \quad (3.61)$$

This induced dipole moment oscillates with the frequency of the incident light-wave:

$$\mu = \alpha \cdot E_0 \cdot \cos(2\pi\nu \cdot t) \quad (3.62)$$

The oscillating dipole creates an electromagnetic wave which spreads radially from the dipole with velocity c . This electromagnetic wave contains components of both electric and magnetic fields, which are perpendicular to each other and to the direction of propagation. At a large enough distance from the dipole, the strength of the electrical field is given by the distance to the dipole, r , and the angle between the direction of propagation and the dipole axis, ϑ . If the field strength of the scattered light is given by E_s :

$$E_s = \frac{1}{4\pi\varepsilon_0 c^2} \cdot \frac{1}{r} \sin \vartheta \cdot \frac{d^2 \mu}{dt^2} \quad (3.63)$$

Substituting (3.62) in (3.63) gives

$$E_s = -\frac{\pi \cdot \alpha \cdot v^2}{\varepsilon_0 c^2} \cdot \frac{1}{r} \sin \vartheta \cdot E_0 \cos(2\pi\nu \cdot t) \quad (3.64)$$

The detector of the light scattering apparatus registers the intensity, i.e., the ratio of the strength of the light impacting on the detector and its area, or, more exactly, the time average of this intensity. This intensity is identical to the product of $\varepsilon_0 c$ and the square of the wave's electrical field strength. Thus, the intensity of the scattered light is given by

$$I = \varepsilon_0 c \cdot \left\langle \left[-\frac{\pi \cdot \alpha \cdot v^2}{\varepsilon_0 c^2} \cdot \frac{1}{r} \sin \vartheta \cdot E_0 \cos(2\pi\nu \cdot t) \right]^2 \right\rangle \quad (3.65)$$

$$I = \left(\frac{\pi \cdot \alpha \cdot v^2}{\varepsilon_0 c^2} \cdot \frac{1}{r} \sin \vartheta \right)^2 \cdot \varepsilon_0 c E_0^2 \cdot \langle \cos^2(2\pi\nu \cdot t) \rangle \quad (3.66)$$

$$I = \left(\frac{\pi \cdot \alpha \cdot v^2}{\varepsilon_0 c^2} \cdot \frac{1}{r} \sin \vartheta \right)^2 \cdot \varepsilon_0 c E_0^2 \cdot \frac{1}{2} \quad (3.67)$$

The intensity of the stimulating wave equals $1/2\varepsilon_0 c E_0^2$ and the relation ν/c is identical to the reciprocal wavelength $1/\lambda_0$. Thus, for the ratio of scattered to incident intensity, I/I_0 ,

$$\frac{I}{I_0} = \frac{\pi^2 \cdot \alpha^2}{\varepsilon_0^2 \lambda_0^4} \cdot \frac{1}{r^2} \sin^2 \vartheta \quad (3.68)$$

In a light scattering experiment, the illuminating light beam and the connecting line from the scattering volume to the detector form a plane. The stimulated wave can now take two marked polarization directions relative to this plane. If the irradiated wave is polarized vertical to the plane (■ Fig. 3.9a), then the angle between the direction of observation and the dipole axis ϑ is always 90° , regardless of the angle θ between the direction of irradiation and that of observation. As a result, for the case of vertical polarization I_\perp :

$$\frac{I_\perp}{I_0} = \frac{\pi^2 \cdot \alpha^2}{\varepsilon_0^2 \lambda_0^4} \cdot \frac{1}{r^2} \quad (3.69)$$

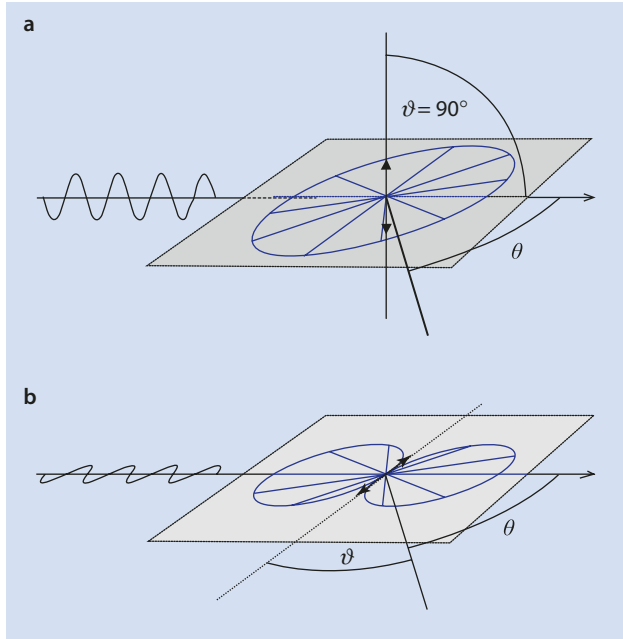
If the irradiated wave is polarized parallel to this plane (■ Fig. 3.9b), then $\vartheta = 90^\circ - \theta$. In this case (scattering intensity for the case of parallel (horizontal) polarization I_\parallel):

$$\frac{I_\parallel}{I_0} = \frac{\pi^2 \cdot \alpha^2}{\varepsilon_0^2 \lambda_0^4} \cdot \frac{1}{r^2} \cos^2 \theta \quad (3.70)$$

If the scattering center is stimulated by non-polarized light, this corresponds to a simultaneous stimulation in both polarization directions and the scattered intensity corresponds to the average of (3.69) and (3.70):

$$\frac{I}{I_0} = \frac{\pi^2 \cdot \alpha^2}{\varepsilon_0^2 \lambda_0^4} \cdot \frac{1}{r^2} \cdot \frac{1 + \cos^2 \theta}{2} \quad (3.71)$$

Fig. 3.9 Dependence of the intensity of the scattered light on the observation angle θ .
(a) Vertical polarization.
(b) Parallel (horizontal) polarization



If it is assumed that

- Not only one, but N scattering centers are present in the stimulated volume V under observation
- The scattering centers are small enough to exclude interference occurring within the scattering centers
- The distances between the scattering centers are large enough
- The centers are distributed arbitrarily in the volume

then the scattering processes can be considered to be mutually independent. In this case, the intensity of the scattered light is given by (3.71) multiplied by the number of scattering centers

$$\frac{I}{I_o} = \frac{\pi^2 \cdot \alpha^2}{\varepsilon_0^2 \lambda_0^4} \cdot \frac{1}{r^2} \cdot \frac{1 + \cos^2 \theta}{2} \cdot N \quad (3.72)$$

If this is divided by those parameters that solely depend on the apparatus (r , θ , and V), one obtains the so-called Rayleigh ratio R_θ , which describes, for example, the scattering of light through dilute gases:

$$R_\theta \equiv \frac{I}{I_o} \frac{r^2}{(1 + \cos^2 \theta) V} = \frac{\pi^2 \cdot \alpha^2}{2 \varepsilon_0^2 \lambda_0^4} \cdot \frac{N}{V} \quad (3.73)$$

Three conclusions can be drawn from (3.73):

- The intensity of the scattered light increases linear to the concentration (number/volume) of the scattering centers, N/V
- The intensity is proportional to the polarizability α of the scattering centers
- The intensity is inversely proportional to the wavelength λ_0

The last point should be familiar from daily life: the sky or faraway mountains appear to be blue because the atmosphere preferentially scatters the short-wavelength rays from the sun laterally and the scattered radiation is superimposed by our perception onto distant objects. If one looks directly at the sun, for example during sunset, it appears to be yellow or red because the scattering preferentially reduces the shorter wavelength parts of the sun's light.

With a knowledge of the polarizability of the scattering centers and their concentration (number), and therefrom the corresponding mass concentration, the molar mass of the centers can be calculated. This is possible, for example, with dilute gases, for which it can be assumed that each atom is a mutually independent scattering center. However, in this case, (3.73) is more likely to be employed to determine the polarizability of the individual molecules or atoms from a knowledge of their number concentration.

If light scattering is not applied to the scattering centers in a dilute gas but rather to a polymer solution, the situation is different in two respects:

1. The electrical field polarizes not only the scattering center, but also its surroundings
2. It cannot be assumed that the scattering centers are mutually independent

To understand the first difference, the influence of a non-conducting medium on an electrical field needs to be considered. If a dielectric is exposed to an external field E_0 , it is polarized and inside it a diminished field E_i prevails:

$$E_i = \frac{E_0}{\varepsilon_r} \quad (3.74)$$

Here the relative permittivity ε_r is a material-specific and, usually, frequency-dependent constant. According to Maxwell, in non-conducting materials, this is equal to the square of the refractive index \tilde{n} :

$$\varepsilon_r = \tilde{n}^2 \quad (3.75)$$

When electromagnetic radiation encounters a non-conductor, the waves penetrate it. The radiation retains the same frequency and its propagation velocity is reduced to a speed $v = c / \tilde{n} = c / \sqrt{\varepsilon_r}$ relative to the speed of light c in a vacuum.

Conceptually, a polymer solution can be divided into closely packed small units of volume $dV = V / N_{SC}$, whose number N_{SC} equals that of the scattering centers. It is assumed that fluctuations in the composition lead to each of these individual elements having a relative permittivity $\varepsilon_r + \delta\varepsilon_r$, which deviates from the permittivity of its surroundings by a small amount, $\delta\varepsilon_r$. An electrical field which interacts with this small volume causes it to be polarized so that, observed from a suitably large distance, it appears as a simple dipole moment whose moment is proportional to the difference of its permittivity and that of its surroundings:

$$\mu = \varepsilon_0 \cdot \delta\varepsilon_r \cdot dV \cdot E \quad (3.76)$$

This means that each of these small volumes can act as scattering centers and that α^2 in (3.73) can be replaced by $(\varepsilon_0 \delta\varepsilon_r dV)^2$. Considering a larger number of scattering centers, the system has to retain the freedom that the permittivity of each and every scattering center may differ from those of its neighbors. Thus, an average value for these deviations needs to be employed and α^2 replaced by $\varepsilon_0^2 \langle \delta\varepsilon_0^2 \rangle dV^2$. Thus the intensity of the scattered

light becomes a function of the variance of the relative permittivity. Next, the dependency of the relative permittivity on composition needs to be defined.

$$\delta\varepsilon_r^2 = \left(\frac{\partial\varepsilon_r}{\partial c_2} \right)^2 \langle \delta c_2^2 \rangle \quad (3.77)$$

However, it is rather time-consuming to determine relative permittivities at the frequencies of the incident light directly. Experimentally, it is considerably easier to determine changes in the refractive index with concentration $\partial\tilde{n}/\partial c_2$ so that for convenience the following equation is employed:

$$\langle \delta\varepsilon_r^2 \rangle = \left(\frac{\partial\varepsilon_r}{\partial\tilde{n}} \right)^2 \left(\frac{\partial\tilde{n}}{\partial c_2} \right)^2 \langle \delta c_2^2 \rangle \quad (3.78)$$

From (3.75) one obtains

$$\frac{\partial\varepsilon_r}{\partial\tilde{n}} = 2\tilde{n} \quad (3.79)$$

Inserting this into (3.73) gives

$$R_\theta = \frac{\pi^2 \cdot 4\tilde{n}^2 \varepsilon_0^2 \left(\frac{\partial\tilde{n}}{\partial c_2} \right)^2 \langle \delta c_2^2 \rangle (dV)^2}{2\varepsilon_0^2 \lambda_0^4} \cdot \frac{N_{SC}}{V} \quad (3.80)$$

$$R_\theta = \frac{\pi^2 \cdot 2\tilde{n}^2 \left(\frac{\partial\tilde{n}}{\partial c_2} \right)^2}{\lambda_0^4} \cdot \langle \delta c_2^2 \rangle dV \quad (3.81)$$

From (3.81) it can be seen that the intensity of the scattered light is a function of the variance of the concentration of the dissolved component. At first glance it may appear irritating that the intensity is also dependent on the arbitrarily selected size of the small scattering volume elements (dV). However, as shown below, this apparent dependency is cancelled out by the variance of the composition increasing as the size of the elements decreases. In almost all areas of chemistry it is an admissible simplification to assume that the density of a gas or the composition of a solution within a given volume is identical and independent of any chosen point within the volume. However, for an understanding of light scattering and polymer solutions it is essential to go into more detail. A strictly even distribution of molecules can only be achieved if they are somehow periodically arranged but this would necessitate allocating the molecules to precisely defined positions in space and would only allow a limited number of distribution possibilities. The highest number of distribution possibilities of molecules in space and thus the largest entropy is attained if we assume that we can find a molecule at every position of this space with the same probability (independent of the proximity of another molecule). Such a purely random distribution results in local variations in density and composition. These may be small

compared to the average density or composition, but they can be exactly described using statistical methods. We now turn again to the concept that the polymer solution is made up of many, closely packed small volume elements dV whereby the number concentration or the molar concentration of the molecules or particles contained in each single sub-volume can be described by a normal distribution whose breadth increases with decreasing size of the sub-volume.

To obtain the variance of the deviation of the concentration from the average concentration $\langle \delta c_2^2 \rangle$ —the product of the square of the deviation δc_2^2 and the probability of this deviation $p(\delta c_2)$ —must be integrated over all possible deviations:

$$\langle \delta c_2^2 \rangle = \int p(\delta c_2) \delta c_2^2 d\delta c_2 \quad (3.82)$$

We receive the probability $p(\delta c_2)$ of a deviation via the corresponding Boltzmann distributions of the changes of the free enthalpy of mixing $\delta \Delta G^m(\delta c_2)$ inferred by the deviation. To make the following equations easier to understand, G is used rather than $\Delta G^m(\delta c_2)$:

$$p(\delta c_2) = \frac{\exp\left\{-\frac{\delta G}{k_B T}\right\} d\delta c_2}{\int \exp\left\{-\frac{\delta G}{k_B T}\right\} d\delta c_2} \quad (3.83)$$

Because all the combined compositions of all the sub-volumes must equal the average composition, the composition of some volumes deviates positively from the average composition whereas others deviate negatively. To simplify, it is assumed that for every sub-volume that deviates from the average composition by the amount δc_2 there exists another sub-volume that deviates from the composition by the opposite amount, $-\delta c_2$. The free enthalpy of mixing of each of these volumes can be written as a Taylor series which is terminated here after the second element. Thus, combining the deviations from the two volumes considered one obtains

$$\delta G = \frac{1}{2} \left[\frac{\partial G}{\partial c_2} \cdot \delta c_2 + \frac{1}{2} \frac{\partial^2 G}{\partial c_2^2} \cdot \delta c_2^2 + \frac{\partial G}{\partial c_2} \cdot (-\delta c_2) + \frac{1}{2} \frac{\partial^2 G}{\partial c_2^2} \cdot (-\delta c_2)^2 \right] \quad (3.84)$$

$$\delta G = \frac{1}{2} \frac{\partial^2 G}{\partial c_2^2} \cdot \delta c_2^2 \quad (3.85)$$

Here the first two terms in the square bracket refer to the first sub-volume and the last two refer to the second sub-volume with opposite deviation. The factor $\frac{1}{2}$ in front of the bracket arises because the change of the free enthalpy for each sub-volume is considered but the terms in parentheses are the sum of the free enthalpies for two sub-volumes.

The two linear terms in the parentheses cancel each other so that, to a first approximation, the deviation of the free enthalpy from the average value is proportional to the square of the deviation.

$$p(\delta c) = \frac{\exp\left\{-\frac{1}{2} \frac{\partial^2 G / \partial c_2^2}{k_B T} \cdot \delta c_2^2\right\} d\delta c_2}{\int \exp\left\{-\frac{1}{2} \frac{\partial^2 G / \partial c_2^2}{k_B T} \cdot \delta c_2^2\right\} d\delta c_2} \quad (3.86)$$

Thus, the function $p(\delta c_2)$ is described by a normal distribution with a variance given by

$$\langle \delta c_2^2 \rangle = \frac{k_B T}{\partial^2 G / \partial c_2^2} \quad (3.87)$$

The next step requires the second derivative of the free enthalpy as a function of concentration. To obtain this it is assumed that the free enthalpy of the system is given by the sum of the chemical potentials of the two substances μ_1 and μ_2 multiplied by their amounts, N_1 and N_2 , respectively:

$$G = \mu_1 N_1 + \mu_2 N_2 \quad (3.88)$$

The derivative with respect to the concentration of the dissolved substance is given by

$$\frac{dG}{dc_2} = N_1 \frac{d\mu_1}{dc_2} + \mu_1 \frac{dN_1}{dc_2} + N_2 \frac{d\mu_2}{dc_2} + \mu_2 \frac{dN_2}{dc_2} \quad (3.89)$$

According to the Gibbs–Duhem equation it holds that

$$N_1 \frac{d\mu_1}{dc_2} + N_2 \frac{d\mu_2}{dc_2} = 0 \Leftrightarrow \frac{d\mu_2}{dc_2} = -\frac{N_1}{N_2} \frac{d\mu_1}{dc_2} \quad (3.90)$$

Thus, the sum of the first and third terms on the right hand side of (3.89) equals zero. Furthermore, for the scattering center at constant volume, dV , one gets:

$$\frac{dc_2}{dN_2} = \frac{d}{dN_2} \frac{M_2 N_2}{dV} = \frac{M_2}{dV} \frac{d}{dN_2} N_2 = \frac{M_2}{dV} \Leftrightarrow \frac{dN_2}{dc_2} = \frac{dV}{M_2} \quad (3.91)$$

$$\frac{dc_2}{dN_1} = \frac{d}{dN_1} \frac{M_2 N_2}{dV} = \frac{M_2}{dV} \frac{d}{dN_1} N_2 = \frac{M_2}{dV} \frac{d}{dN_1} \frac{dV - \bar{V}_1 N_1}{\bar{V}_2} \quad (3.92)$$

$$\frac{dc_2}{dN_1} = -\frac{\bar{V}_1}{\bar{V}_2} \frac{M_2}{dV} \Leftrightarrow \frac{dN_1}{dc_2} = -\frac{\bar{V}_2}{\bar{V}_1} \frac{dV}{M_2} \quad (3.93)$$

Thus, from (3.89)–(3.92):

$$\frac{dG}{dc_2} = \left(\mu_2 - \frac{\bar{V}_2}{\bar{V}_1} \mu_1 \right) \frac{dV}{M_2} \quad (3.94)$$

Differentiating (3.94) with respect to c_2 yields

$$\frac{d^2G}{dc_2^2} = \left(\frac{d}{dc_2} \mu_2 - \frac{\bar{V}_2}{\bar{V}_1} \frac{d}{dc_2} \mu_1 \right) \frac{dV}{M_2} \quad (3.95)$$

Applying the Gibbs–Duhem equation (3.90) once more, one obtains

$$\frac{d^2G}{dc_2^2} = - \left(\frac{N_1}{N_2} + \frac{\bar{V}_2}{\bar{V}_1} \right) \frac{dV}{M_2} \frac{d\mu_1}{dc_2} = - \frac{N_1\bar{V}_1 + N_2\bar{V}_2}{N_2\bar{V}_1} \frac{dV}{M_2} \frac{d\mu_1}{dc_2} \quad (3.96)$$

$$\frac{d^2G}{dc_2^2} = - \frac{N_1\bar{V}_1 + N_2\bar{V}_2}{N_2M_2} \frac{dV}{\bar{V}_1} \frac{d\mu_1}{dc_2} = - \frac{1}{c_2} \frac{dV}{\bar{V}_1} \frac{d\mu_1}{dc_2} \quad (3.97)$$

Assuming that the chemical potential is dependent on the concentration, concentration-dependent activity constants could be inserted. However, when deriving the theory for osmometry, an alternative approach was used. Thus, deviation from ideal behavior was described with the aid of virial coefficients. The same approach can be made in this case. From the equation

$$\mu_1 = \mu_1^\circ + RT \cdot \bar{V}_1 \left(\frac{1}{M_2} \cdot c_2 + A_2 \cdot c_2^2 + A_3 \cdot c_2^3 + \dots \right), \quad (3.98)$$

it follows that

$$\frac{d\mu_1}{dc_2} = RT \cdot \bar{V}_1 \left(\frac{1}{M_2} + 2A_2 \cdot c_2 + 3A_3 \cdot c_2^2 + \dots \right) \quad (3.99)$$

and

$$\frac{d^2G}{dc_2^2} = \frac{dV}{c_2} RT \left(\frac{1}{M_2} + 2A_2 \cdot c_2 + 3A_3 \cdot c_2^2 + \dots \right) \quad (3.100)$$

If (3.100) is combined with (3.87) one obtains

$$\langle \delta c^2 \rangle = \frac{c_2}{N_A \left(\frac{1}{M_2} + 2A_2 \cdot c_2 + 3A_3 \cdot c_2^2 + \dots \right)} \frac{1}{dV} \quad (3.101)$$

Substituting (3.101) into (3.80) yields

$$R_\theta = \frac{4\pi^2}{\lambda_0^4} \tilde{n}^2 \left(\frac{\partial \tilde{n}}{\partial c} \right)^2 \frac{1}{N_A} \cdot \frac{c_2}{\left(\frac{1}{M_2} + 2A_2 \cdot c_2 + 3A_3 \cdot (c_2)^2 + \dots \right)} \quad (3.102)$$

The value of (3.102) can be more easily appreciated by introducing an optical constant K , whereby

$$K = \frac{4\pi^2}{\lambda_0^4 N_A} \bar{n}^2 \left(\frac{\partial \bar{n}}{\partial c} \right)^2, \quad (3.103)$$

so that (3.102) becomes

$$K \frac{c_2}{R_\theta} = \frac{1}{M_2} + 2A_2 \cdot c_2 + 3A_3 \cdot (c_2)^2 + \dots \quad (3.104)$$

Not only does (3.104) corroborate the expectation that the ratio of the scattering intensity and concentration should increase proportional to the size of the dissolved molecules; it also permits the quantitative determination of the molar mass of the scattering particles. Because solutions are rarely ideal, considerable dilution is necessary to ensure that the non-ideal effects are negligible. For very dilute solutions (3.104) reduces to

$$K \cdot \lim_{c_2 \rightarrow 0} \left(\frac{c_2}{R_\theta} \right) = \frac{1}{M_2} \quad (3.105)$$

In practical experiments, the signal/noise ratio deteriorates with concentration so that the scattering intensities are determined for a range of concentrations and the results fitted to the above polynomial equation and this extrapolated to $c_2=0$. In most cases, a straight line fitted to the data points at lowest concentrations suffices for a useful result. This method not only gives the molar mass of the dissolved substance; by determining the osmotic pressure from the virial coefficient, information about the quality of the solvent can also be obtained.

If the polymer does not have a singular molar mass, it is interesting to consider the following rearrangement of (3.105):

$$1 = K \cdot \lim_{c_2 \rightarrow 0} \left(\frac{c_2 M_2}{R_\theta} \right) \quad (3.106)$$

For a polymer with a distribution of molar mass, the contribution of each of the components to the scattering intensity can be considered as additive so that

$$1 = K \cdot \lim_{\sum c_i \rightarrow 0} \left(\frac{1}{R_\theta} \sum c_i M_i \right) = K \cdot \lim_{\sum c_i \rightarrow 0} \left(\frac{\sum c_i}{R_\theta} \cdot \frac{\sum c_i M_i}{\sum c_i} \right) \quad (3.107)$$

$$1 = K \cdot \lim_{\sum c_i \rightarrow 0} \left(\frac{\sum c_i}{R_\theta} \frac{\sum m_i M_i}{\sum m_i} \right) = K \cdot \lim_{\sum c_i \rightarrow 0} \left(\frac{\sum c_i}{R_\theta} M_w \right) \quad (3.108)$$

$$1 = K \cdot \lim_{c_2 \rightarrow 0} \left(\frac{c_2}{R_\theta} M_w \right) = K \cdot \lim_{c_2 \rightarrow 0} \left(\frac{c_2}{R_\theta} \right) \cdot M_w \quad (3.109)$$

Thus, static light scattering does not yield a number average molar mass as the other methods described above, but a weight average molar mass.

Up to this point it has been assumed that the dissolved molecules are small compared to the wavelength of the employed light. For particles whose size is larger than $\lambda/20$ it is necessary to take into account that radiation is emitted from various regions of the particle and that the different portions of radiation interfere with each other (■ Fig. 3.10). Scattering

in the same direction as the incident light, i.e., at a scattering angle of approximately zero, all components of this scattered light are in phase and interfere constructively. Lateral scattering leads to phase shifts between the different components and the scattered light is reduced *depending on the angle*.

The dependency of the scattering intensity on the scattering angle is specific to the shape of the molecule or particle. This can be expressed by multiplying the intensity of the scattered light with an angle-dependent factor, the so-called form factor.

At least for spherically symmetrical objects it is relatively easy to derive the form from the dependence of scattering intensity on the scattering angle. If two waves of the same amplitude E and identical wavelength λ originate from two points offset against each other in the direction of the direction of propagation x by a line segment S , they can be added together using the rules of addition for trigonometric functions to give a wave whose amplitude depends on the offset S according to

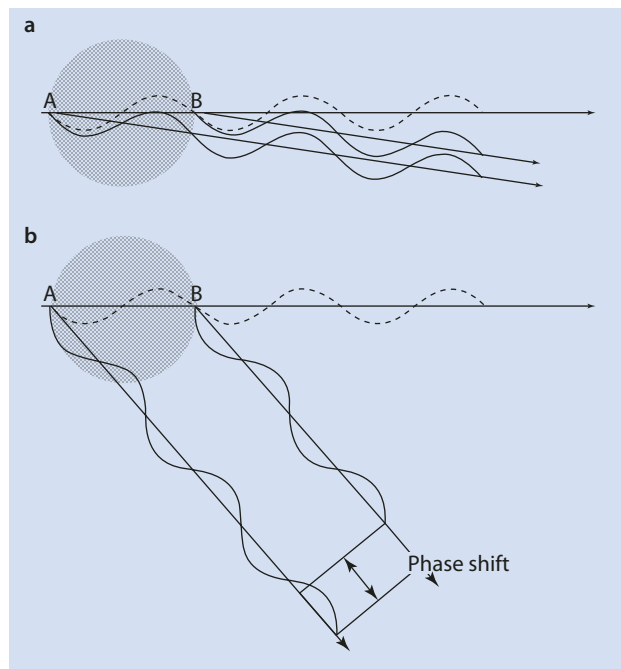
$$E \sin \left[\frac{2\pi}{\lambda} \left(x - \frac{S}{2} \right) \right] + E \sin \left[\frac{2\pi}{\lambda} \left(x + \frac{S}{2} \right) \right] = 2E \sin \left[\frac{2\pi}{\lambda} x \right] \cdot \cos \left[\frac{2\pi}{\lambda} \frac{S}{2} \right] \quad (3.110)$$

The ratio of the amplitude at negligible offset, E^* , and the interference reduced amplitude, E , is given by

$$\frac{E}{E^*} = \cos \left[\frac{2\pi}{\lambda} \frac{S}{2} \right] \quad (3.111)$$

The geometry of light scattering by a large object can be explained as shown in (■ Fig. 3.11a). It is observed that all waves which originate from a plane along a single line parallel with

■ **Fig. 3.10** Scattered light in different regions because of a "large" object. **(a)** Negligible phase difference where the scattering angle is close to zero. **(b)** Dependent on the angle and no longer negligible when the scattering angle is considerably larger than zero. This leads to destructive interference so that the scattering intensity is reduced and dependent on the scattering angle



half the observation angle (dashed line), are in phase—the line segment \overline{PO} has the same length as the line segment $\overline{PO'}$. Waves that originate from a plane lying parallel to this plane, but shifted by a distance Δx (e.g., the dotted line), compared to waves which originate from the first plane, are phase shifted by an amount S :

$$S = \overline{O'Q} + \overline{QO''} = d \sin(\theta/2) + d \sin(\theta/2) = 2d \sin(\theta/2) \quad (3.112)$$

The simplest symmetrical, spherical object is a hollow sphere with extremely thin walls and uniform density (symbolized by the gray circle in [Fig. 3.11b](#)). Such a hollow sphere can be divided into rings lying parallel to a plane which cuts the center of the hollow sphere (represented by the dashed line in [Fig. 3.11b](#)) and halves the observation angle. Two of these rings (symbolized by dotted lines in [Fig. 3.11b](#)) at an equal distance in front of or behind this plane have an identical circumference. The interference of the radiation scattered by each pair of rings leads to a radiation which is in phase with the radiation scattered by the plane represented by the dashed line. Thus, the amplitude of the radiation originating from each of the pairs can be initially determined and this can then be integrated over all rings. Each pair of rings contributes to the scattering radiation with an intensity proportional to the ratio of the area of the ring-pair to the total area of the sphere, multiplied by the reduction caused by interference according to (3.110). If the radius of the sphere is designated as R and the half apex angle of a cone connecting the center of the sphere with the ring, as α , then the circumference of the ring is given by $2\pi R \sin \alpha$, its breadth by $R d\alpha$, and its area by $R^2 \sin \alpha d\alpha$. As the geometry is mirror-symmetrical, the integration needs only to be made over one hemisphere. The surface area of a hemisphere is equal to $2\pi R^2$. Therefore for a hollow sphere:

$$\frac{E}{E^*} = \int_{\alpha=0}^{\pi/2} \frac{\cos\left[\frac{2\pi S}{\lambda} \frac{S}{2}\right] \cdot 2\pi R \sin \alpha \cdot R d\alpha}{2\pi R^2} = \int_{\alpha=0}^{\pi/2} \cos\left[\frac{2\pi S}{\lambda} \frac{S}{2}\right] \sin \alpha \cdot d\alpha \quad (3.113)$$

$$\frac{E}{E^*} = \int_{\alpha=0}^{\pi/2} \cos\left[\frac{2\pi}{\lambda} \frac{2 \cdot 2R \cdot \cos \alpha \cdot \sin(\theta/2)}{2}\right] \sin \alpha d\alpha \quad (3.114)$$

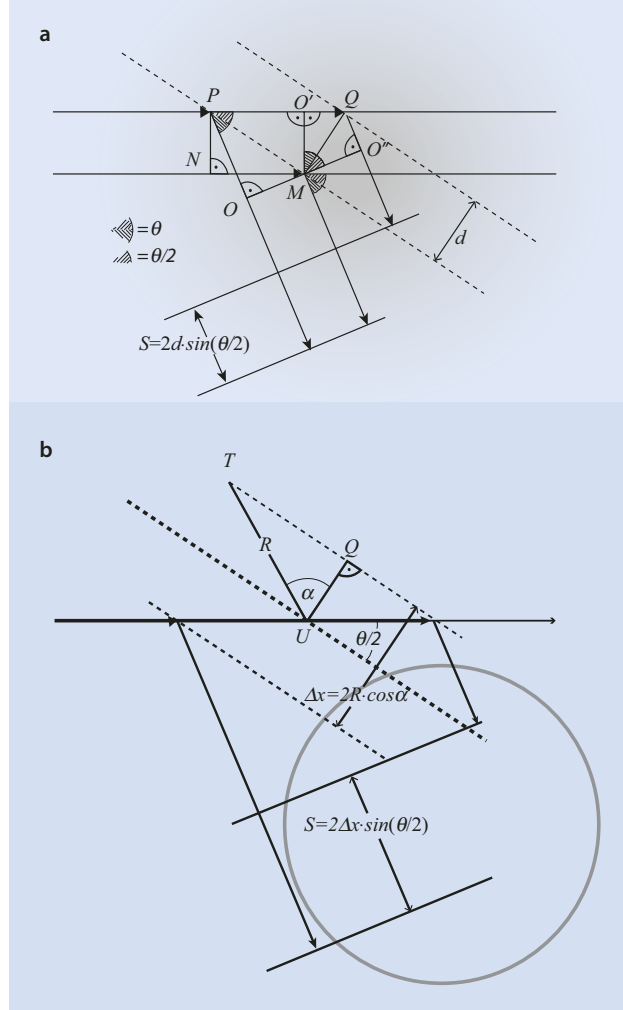
$$\frac{E}{E^*} = \int_{\alpha=0}^{\pi/2} \cos[qR \cdot \cos \alpha] \sin \alpha d\alpha \quad (3.115)$$

$$\frac{E}{E^*} = \int_{\alpha=0}^{\pi/2} \cos[qR \cdot \cos \alpha] \sin \alpha d\alpha \quad (3.116)$$

where the value of the scattering vector q is given by

$$q = \frac{4\pi \tilde{n}}{\lambda_0} \sin(\theta/2) = \frac{4\pi}{\lambda} \sin(\theta/2) \quad (3.117)$$

Fig. 3.11 (a) Geometrical demonstration of phase differences as a function of scattering angle. (b) Alternative approach to the geometric relationships (see text for explanation)



Although the integral in (3.116) looks quite complicated with its nested trigonometric functions, it can be solved relatively easily by introducing the substitution

$$a = qR \cdot \cos \alpha \tag{3.118}$$

Because

$$\frac{da}{d\alpha} = -qR \cdot \sin \alpha \Leftrightarrow d\alpha = -\frac{1}{qR \cdot \sin \alpha} da \tag{3.119}$$

and applying the integration limits

$$a(\alpha = 0) = qR, \quad a\left(\alpha = \frac{\pi}{2}\right) = 0 \tag{3.120}$$

the integral in (3.116) reduces to

$$\frac{E}{E^*} = \int_{a=qR}^0 \cos a \cdot \sin \alpha \left(-\frac{1}{qR \cdot \sin \alpha} \right) da = -\frac{1}{qR} \int_{a=qR}^0 \cos a \cdot da \quad (3.121)$$

$$\frac{E}{E^*} = -\frac{1}{qR} (\sin 0 - \sin qR) = \frac{\sin qR}{qR} \quad (3.122)$$

The objective is to find a method to eliminate the effects of interference. It is known that these effects become negligible in the limiting case when the angle of scattering is zero so what is needed is an equation relating the scattering intensity and the angle of scattering which can be extrapolated to zero, the value of which cannot be directly measured. Obviously, it is the small scattering angles which need to be examined. In the limiting case, qR approaches zero so that three approaches are possible.

The first approach is to expand $\sin qR$ as a series truncated after the third element:

$$\sin qR = qR - \frac{1}{3!}(qR)^3 \quad (3.123)$$

$$\frac{E}{E^*} = \frac{qR - \frac{1}{3!}(qR)^3}{qR} = 1 - \frac{1}{6}R^2q^2 \quad (3.124)$$

Because the intensity is proportional to the square of the amplitude ($I = |E|^2$), the second approach makes the approximation that qR is extremely small so that the form factor $P(q)$ can be given by

$$\frac{I}{I^*} = \left(1 - \frac{1}{6}R^2q^2 \right)^2 = 1 - \frac{1}{3}R^2q^2 + \frac{1}{36}R^4q^4 \approx 1 - \frac{1}{3}R^2q^2 = P(q) \quad (3.125)$$

For the third approach, the approximation $1/(1-x) \approx 1+x$ is made so that

$$\frac{I^*}{I} = \frac{1}{P(q)} \approx 1 + \frac{1}{3}R^2q^2 \quad (3.126)$$

The transition from a hollow sphere to any symmetrical spherical solid is now simple. The sphere can simply be built up from concentric spheres in which the local concentration of polymer segments, $c(R)$, is a function of the radius, and integrate over the radii:

$$\frac{1}{P(q)} \approx 1 + \frac{1}{3}q^2 \frac{\int_{R=0}^{\infty} R^2 c(R) 4\pi R^2 dR}{\int_{R=0}^{\infty} c(R) 4\pi R^2 dR} \quad (3.127)$$

The quotient of integrals in (3.127) is called the square of the radius of gyration r_G . Here the radius of gyration—as is the norm in polymer science—is defined by the average

square distance from the center of gravity of the object. However, in engineering it is the norm to define the radius of gyration by the average square distance from a defined axis of rotation. It is important not to confuse these two definitions.

By inserting the radius of gyration into (3.127) one obtains

$$\frac{1}{P(q)} \approx 1 + \frac{1}{3} q^2 r_G^2 \quad (3.128)$$

It can be shown that (3.128) is also valid for spherically asymmetrical objects, e.g., cylinders, ellipsoids, or discs, but the mathematical proof is not given here. The “trick” of observing pairs of planes at equal distances from the center of the object and limiting observations to small scattering angles serve as a logical explanation that all further observations of the interferences lead simply to additive combinations of the corresponding intensities. In this way, the scattering of a number of different objects can be treated as the scattering by uniform objects of an averaged shape. The sum of asymmetrical spherical objects scattered in space with no predominant orientation act, on average, as symmetrical spherical objects with identical radii of gyration.

With the form factor $P(q)$, in analogy to (3.104) and (3.105):

$$K \frac{c_2}{R_\theta} = \frac{1}{M_2 P(q)} + 2A_2 \cdot c_2 + 3A_3 \cdot (c_2)^2 + \dots \quad (3.129)$$

and

$$K \cdot \lim_{c_2 \rightarrow 0} \left(\frac{c_2}{R_\theta} \right) = \frac{1}{M_2 P(q)} \quad (3.130)$$

Inserting (3.128) leads to

$$K \frac{c_2}{R_\theta} \approx \frac{1}{M_2} \left(1 + \frac{1}{3} q^2 r_G^2 + \dots \right) + 2A_2 c_2 + 3A_3 (c_2)^2 + \dots \quad (3.131)$$

$$K \cdot \lim_{c_2 \rightarrow 0, q \rightarrow 0} \left(\frac{c_2}{R_\theta} \right) = \frac{1}{M_2} \quad (3.132)$$

Equations (3.128) and (3.131) are the quintessence of this section. To eliminate the effect of interference by extrapolating to a zero scattering angle, a graph of Kc_2/R_θ vs q^2 or $\sin^2(\theta/2)$ gives a straight line ably suitable for extrapolation to $\theta=0$. For polydisperse samples, light scattering yields a weight average molar mass M_w .

Experimental Execution and Evaluation of the Measurements

As discussed above, with this method the light scattered by a polymer solution is measured at different observation angles. The refraction increment $d\bar{n}/dc_2$ is determined from separate measurements. To eliminate non-ideal effects, measurements are made over a range of concentrations.

From the results of the previous section, the following equation, the so-called *Zimm equation*, can be derived for vertically polarized incident light using (3.73). This equation describes the intensity of light scattered by polymer solution:

$$\frac{4\pi^2 \cdot \tilde{n}^2}{N_A \cdot \lambda_0^4} \cdot \left(\frac{d\tilde{n}}{dc_2} \right)^2 \cdot \frac{c_2}{R_\theta} = \frac{1}{M_w} \left(1 + \frac{16\pi^2 \tilde{n}^2}{3\lambda_0^2} \cdot \sin^2(\theta/2) \cdot r_G^2 \right) + 2A_2 \cdot c_2 \quad (3.133)$$

For the purpose of clarity, the definitions of the symbols are listed again here:

\tilde{n}	Refractive index of the solvent
N_A	Avogadro's constant
λ_0	Wavelength of light in vacuum
$d\tilde{n}/dc_2$	Refractive index increment
c_2	Concentration of the dissolved substance
R_θ	Experimentally defined Raleigh ration (see below)
M_w	Weight average molar mass
θ	Scattering angle
r_G	Radius of gyration of the polymer chain
A_2	Second virial coefficient

The Raleigh ratio of the sample—the actual experimental measurement result of the light scattering experiment—is usually obtained by subtracting the measured scattering intensities of the solvent I_1 from those of the solution I_2 ; additionally, the Raleigh ratio is normalized using the ratio of a standard R_{stand} (nowadays generally toluene) determined at the wavelength being employed:

$$R_\theta = \frac{I_2 - I_1}{I_1} R_{stand} \quad (3.133a)$$

Furthermore, the parameters dependent on the device and the solvent are combined in the optical constant K (cf. (3.103)):

$$K = \frac{4\pi^2}{\lambda_0^4 N_A} \tilde{n}^2 \left(\frac{\partial \tilde{n}}{\partial c} \right)^2 \quad (3.133b)$$

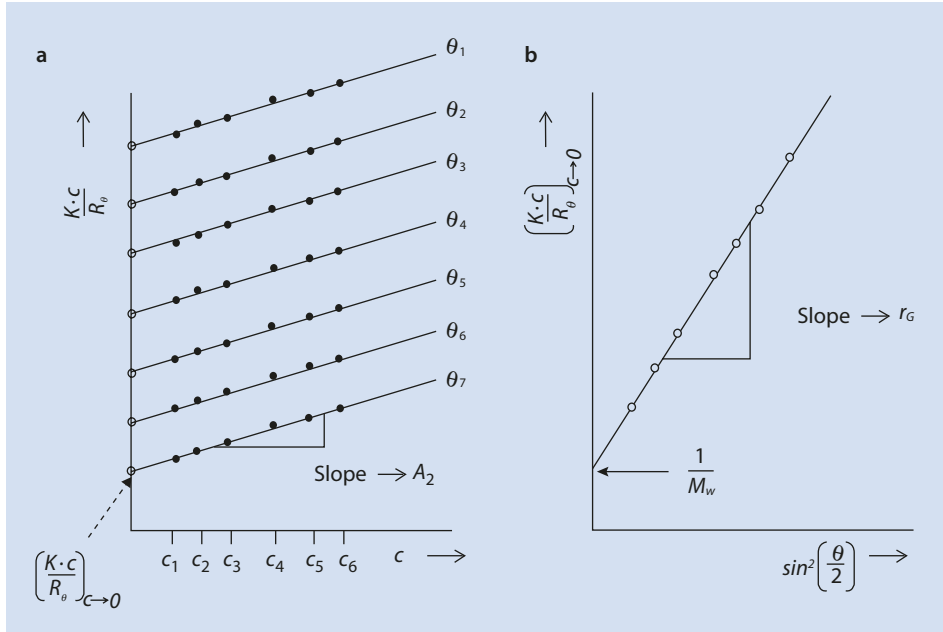
If the scattering vector (cf. (3.117)) is also employed:

$$q = \frac{4\pi \tilde{n}}{\lambda_0} \sin(\theta/2) = \frac{4\pi}{\lambda} \sin(\theta/2), \quad (3.133c)$$

The Zimm equation (cf. (3.104)) is now much simpler:

$$\frac{Kc_2}{R_\theta} = \frac{1}{M_w} \left(1 + \frac{1}{3} \cdot q^2 \cdot r_G^2 \right) + 2A_2 \cdot c_2 \quad (3.134)$$

To obtain the molar mass of the substance being analyzed from light scattering data, the Raleigh ratio R_θ at various concentrations and angles needs to be determined and



■ **Fig. 3.12** Twofold extrapolation for a set of light scattering data. (a) Extrapolation to a zero concentration $c_2=0$. (b) Then to a scattering angle $\theta=0$. c Polymer concentration c_i , indices indicate different polymer concentrations

extrapolated to $\theta=0$ and $c_2=0$; the sequence of the procedure is not important. This procedure is summarized in ■ Fig. 3.12.

As a “by-product” of this evaluation, the gradients of the linear extrapolations result in the radius of gyration r_G and the second virial coefficient A_2 . The radius of gyration determined in this way is the z-average of the squares of the radii of gyration.

With the aid of modern data evaluation programs, the visualization of the light scattering data as a perspective projection of a three-dimensional diagram is trivial and customizing a plane directly onto the light scattering data according to (3.131) is easily achieved. However, in this case it is easy to lose sight of any deviations of the experimental data from the expected linearity. A good compromise is the so-called Zimm plot which comes close to the visual appearance of the 3D projection but allows an exact graphical evaluation (■ Fig. 3.13). In this diagram, Kc_2/R_θ is plotted against the sum of $\sin^2(\theta/2)$ and the polymer concentration c_2 , whereby the latter is multiplied by a more or less randomly selected constant k to simplify the extrapolation. The constant k is chosen in such a way that the data points are equally distributed across the diagram but its value does not influence the result. All data points that belong to different angles but the same concentration c_{2i} are connected by one line. On this line, the position at which the lateral position is $k \cdot c_{2i}$ is marked. This corresponds to an extrapolation to $\sin^2(\theta/2)=0$. The resulting dots are connected by a further line, which is extended to the ordinate. The gradient of this line is $2A_2 \cdot k$, its intercept with the ordinate is identical to an extrapolation to $c_2=0$ and $\sin^2(\theta/2)=0$ and has the value of $1/M_w$. The same procedure is then executed again in reverse. A line is drawn through all dots that belong to a given angle θ_p but to different concentrations, on which the lateral positions of $\sin^2(\theta/2)$ are

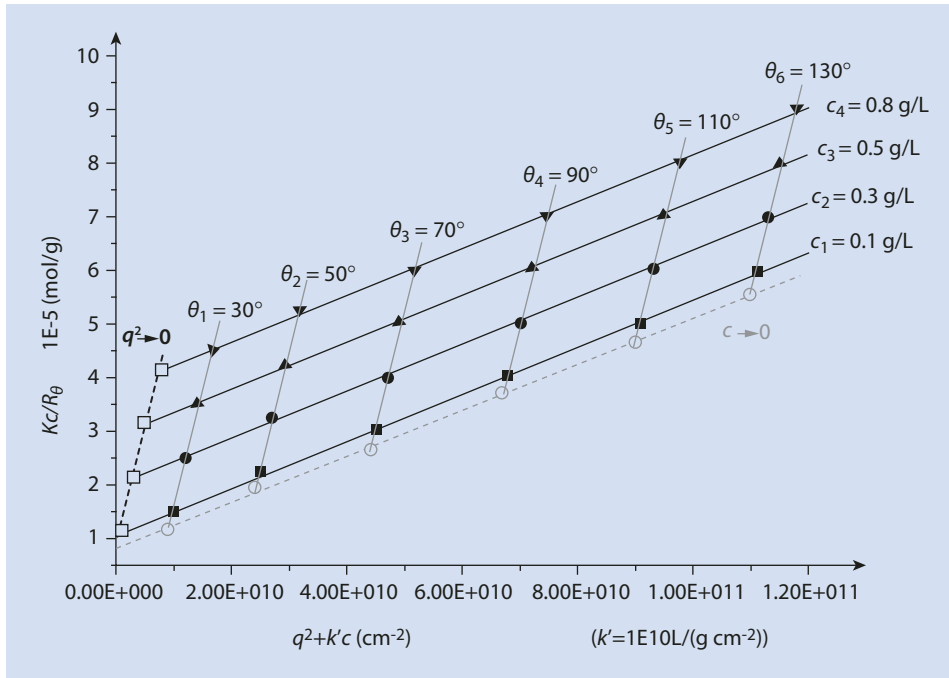


Fig. 3.13 Zimm-diagram from light scattering measurements on a polymer in toluene. The extrapolations yield the molar mass $M_w = 121$ kg/mol, the radius of gyration $r_G = 124$ nm, and the second virial coefficient $A_2 = 2.2 \cdot 10^{-4}$ mol cm³ g⁻². c polymer concentration c_i indices refer to the different polymer concentrations

marked. These markings are identical to an extrapolation onto $c_2=0$ at a constant scattering angle. A line is again drawn through the resulting dots and extended to the ordinate. The gradient of this line equals $r_G^2 \cdot (4\pi / \lambda)^2 (3M_w)$, its intercept with the ordinate should be the same as that for the previously drawn line and has the value of $1/M_w$.

Thus, not only information about the molar mass of the solute can be obtained from the Zimm plot; the radius of gyration and the second virial coefficient of the osmotic pressure can also be determined. The static light scattering thus offers with a single method the molar mass and also information about the size of the polymer coil in the solution as well as information about the quality of the solvent.

The scattering intensity is measured, e.g., with a photomultiplier or a photo diode. For light scattering measurements the sample solution is irradiated with incident light in a cylindrical cuvette. The intensity of the scattered light is then measured at selected scattering angles θ . In many cases, argon ion lasers ($\lambda_0 = 488$ nm), helium-neon lasers ($\lambda_0 = 633$ nm), or NdYAG solid state lasers ($\lambda_0 = 532$ nm) are used as light sources.

Typically, solutions with concentrations between 0.1 and 0.5 g/L are measured. Interference from impurities, especially from dust particles, must be carefully prevented and the measured values are compared to those of the dust-free solvent.

3.2.6.2 Dynamic Light Scattering

In contrast to static light scattering, in which the scattered light is measured over relatively long time periods and time averaged values of the scattering intensity obtained, for dynamic light scattering the fluctuation of the scattering with time is measured—the "noise." Because of the complexity of this measurement method we only elaborate the basic principles here.

As shown in [Fig. 3.8](#), the incident and the scattered light beams form a plane. The detector therefore only determines the scattering intensity of those scattering centers which are in the volume defined by the overlap of the incident and the scattered light beams. This volume is comparatively small. The diffusion of the polymers in the scattering volume leads to fluctuations in intensity over time. Resolution of these intensity fluctuations with respect to time gives a measure of the speed at which the polymers diffuse through the solution and thus also within the scattering volume. Thus, this method allows direct determination of the diffusion coefficient of the dissolved macromolecules which has been discussed in connection with the ultracentrifuge ([▶ Sect. 3.2.5.2](#)).

For further information the interested reader is referred to the specialist literature (e.g., [Schaertl 2007](#)).

3.2.7 MALDI-TOF-MS

3.2.7.1 General

The **Matrix Assisted Laser Desorption Ionization Time of Flight Mass Spectroscopy** (MALDI-TOF-MS) is a fast and sensitive absolute method for determining both the number average and weight average molar masses. It has a special status in the analysis of polymers of biological origin. In an ideal case, molar masses of <300,000 g/mol can be measured with an accuracy of $\pm 0.01\%$ ([Pasch and Schrepp 2003](#)).

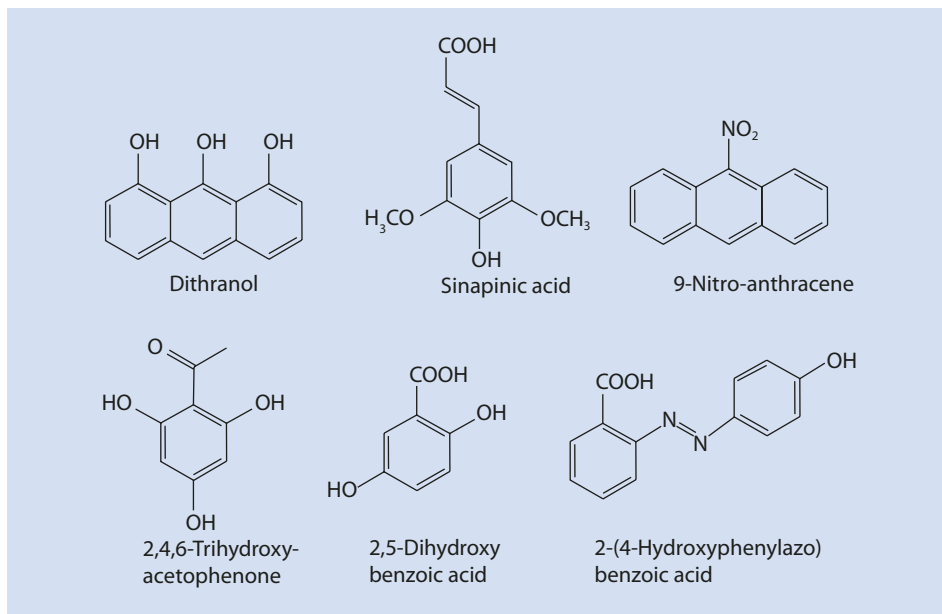
3.2.7.2 Basics

For the measurement the polymer is dissolved in a solution with an approx. 1000-fold excess of an organic matrix. Typical matrix molecules are presented in ([Fig. 3.14](#)).

After that the solvent is evaporated and, as the matrix crystallizes, the polymer molecules become isolated. This isolation is an important prerequisite for the success of the molar mass determination with MALDI-TOF-MS. In a high vacuum (10^{-6} to 10^{-8} mbar) a short laser pulse is directed onto the sample via special optics. Typically, nitrogen lasers with a wavelength of $\lambda = 337$ nm are used. The matrix strongly absorbs at the wavelength of the laser and the energy absorbed leads to an explosive phase transition of the matrix and the macromolecules into the gas phase.

As well as facilitating the absorption of the energy, the matrix also induces ionization. Electrically charged macromolecules are created by proton transfer in the gas phase. Alternatively, a cation-generating salt (typically a silver, sodium or potassium salt) is often added to the original solution, especially for measurements on synthetic polymers.

The ions generated are then accelerated in an electrostatic field with a strength of 10 to a few 1000 V/mm ([Fig. 3.15](#)). The mass analysis follows with the aid of a time-of-flight analyzer ([Fig. 3.15](#)). For this purpose, the time is determined which the ions need to



■ Fig. 3.14 Typical matrix molecules. Dithranol (also known as anthralin and Cignolin) is shown in its enol-form which is in tautomeric equilibrium with the keto-form

travel across a defined, field-free flight distance between the accelerating electrode (3) and the detector (4). From the flight time, the relation of mass to electric charge of the molecules can be determined. As the MALDI-TOF-MS typically leads to singularly charged ions (the detailed mechanisms are still being discussed), the result is the corresponding molar mass.

Applying the voltage U , according to the principle of energy conservation, gives for the kinetic energy of the ions E_{kin} :

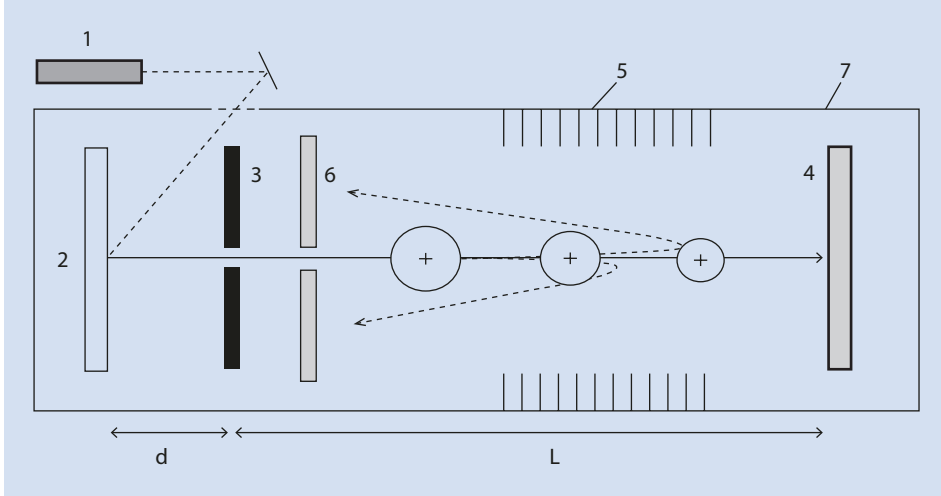
$$E_{kin} = \frac{m \cdot \bar{v}^2}{2} = z \cdot e \cdot U \quad (3.135)$$

m	Mass of the particles
\bar{v}	Average particle velocity
z	Ion charge number
e	Elementary charge
U	Velocity voltage

The velocity reached results from

$$v = a t_{acc} \quad (3.136)$$

a	Acceleration
t_{acc}	Time of acceleration



■ **Fig. 3.15** Setup of a time-of-flight analyzer. (1) Laser, (2) sample holder, (3) accelerating electrode, (4) linear-detector, (5) reflectron, (6) reflectron-detector, (7) vacuum chamber, d acceleration section, L field-free flight distance (linear), (dashed line) flight routes (for the function of the optional reflectron, ion mirrors – see text)

With an acceleration distance d where

$$d = \frac{a}{2} t_{acc}^2 \quad (3.137)$$

the time of acceleration is

$$t_{acc} = d \sqrt{\frac{2m/z}{Ue}} \quad (3.138)$$

The resulting duration of the time taken t_{drift} to cross the field-free distance L is given by

$$t_{drift} = \frac{L}{v} = L \sqrt{\frac{m/z}{2Ue}} \quad (3.139)$$

For the total time of flight:

$$t = t_{acc} + t_{drift} = const \cdot \sqrt{\frac{m}{z}} \quad (3.140)$$

from which, after rearrangement one obtains:

$$\frac{m}{z} = const' \cdot t^2 \quad (3.141)$$

Equations (3.140) and (3.141) are the basic equations of the MALDI-TOF-MS. Because $m \sim t^2$, heavy particles reach the detector later than light ones. Typical times of flight are of the order of milliseconds.

A particularly successful mass resolution is achieved by applying optional reflectors based on an electrical field. Because of the duration of a laser pulse, ions which leave the ion source have neither the same initial energy nor the same kinetic energy. This reduces the resolution. The reflectors help to compensate for the range of energies and for molecules with the same mass to charge ratio. Thus, ions of higher energy penetrate the electrostatic field to a greater depth than those of lower energy. Faster ions therefore take a longer route. After being reflected (*ion mirrors*), ions of identical mass, but with different velocity, are redirected and finally reach the detector at the same time. With this energy focusing, considerable improvements in resolution can be obtained compared to instruments without reflectors.

Example

The capability of MALDI-TOF-MS is best demonstrated by looking at an example.

Figure 3.16 shows the analysis of a polystyrene from a dithranol (Fig. 3.14) matrix containing a silver salt as cation generating agent.

The peaks are easily identified. They can be assigned to individual chains of different mass (in this case, z equals 1). The molar mass of the individual chains are separated by the mass of a single styrene unit. From these peaks and knowledge about the cation generating salt, it is possible to determine the molar mass of the end groups. Furthermore, by integration over all the peaks, an average molar mass can be obtained. When determining the average molar mass it is important to note that the higher molar mass ions may be underrepresented, especially for broader distributions, because of peak broadening and effects dependent on the matrix and the cation generating salt so that the average value can be distorted.

3.3 Relative Methods

Molar mass determinations by methods which do not involve direct, physical-chemical correlation which can be mathematically explained between the actual measurements and the molar mass of the sample are referred to as relative methods. Such methods require a calibration by samples of known molar mass. It is important for this calibration that, among other things, it is known how the molar mass of the calibration standard has been measured and which average value has been determined. Precision demands that calibration should only be carried out using strictly monodisperse standards. However, in practice, such standards are rarely available. It is worth remembering here that even a sample with a polydispersity index of 1.04, which is seen in standard literature as a narrow distribution and may even be considered as monodisperse, still has a molar mass standard deviation of 20% (► Sect. 3.1) so that M_n and M_w are not identical. Thus, if the calibration involves samples whose molar mass was determined by a method which generates, for example, number average M_n , the calibration is not the same as that obtained using sam-

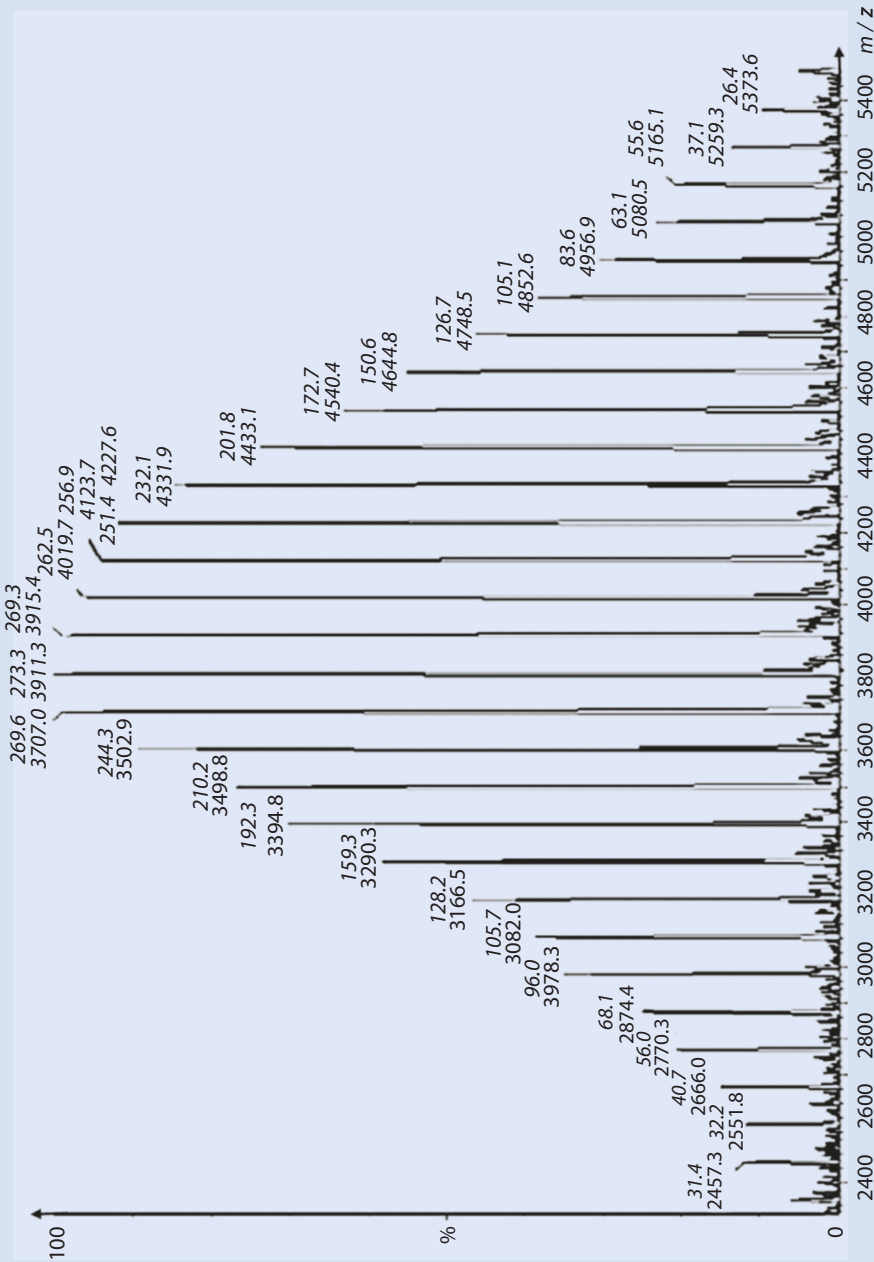


Fig. 3.16 MALDI-TOF-MS-spectrum of a polystyrene. The relative abundance (normalized to the most abundant peak) is plotted against the mass/charge ratio (m/z). The numbers above the peaks are the relative abundance and the corresponding m/z value

ples whose weight average is known.² Strictly speaking, the nature of the calibration samples and how their molar mass was determined belongs to the description of the calibration. Such problems do not arise if strictly monodisperse standards are employed because for such samples the number and weight average molar mass are identical. The most important relative methods which are of greatest practical relevance are size exclusion or gel permeation chromatography (SEC or GPC) and viscometry.

3.3.1 Viscometry

Compared to pure solvents, polymer solutions have higher viscosities. This effect depends on both the concentration of the polymer and its molar mass and remains measurable even for very dilute solutions in which the polymer chains are no longer entangled.

Before evaluating the measured values, it is necessary to define a few terms.

The relative viscosity η_{rel} of a polymer solution with a concentration c_2 is the quotient of the viscosity of the polymer solution η and the pure solvent η_0 :

$$\eta_{rel} = \frac{\eta}{\eta_0} = \frac{t}{t_0} \quad (3.142)$$

This quotient is identical to the quotient of the experimentally measured times t and t_0 , which a solution or the pure solvent require to flow through capillaries, respectively (details can be found below). The relative viscosity, as can be seen from the definition, is dimensionless. It is a measure of the increase in viscosity of a solution compared to that of the pure solvent at a given temperature.

The specific viscosity (also dimensionless) is a measure for the contribution of the polymer to the viscosity of a solution. It is calculated from the quotient of the *difference* in viscosity and the viscosity of the pure solvent:

$$\eta_{sp} = \frac{\eta - \eta_0}{\eta_0} = \frac{\Delta\eta}{\eta_0} \quad (3.143)$$

The reduced viscosity (of unit mL/g and, in older literature, dL/g) is simply the specific viscosity normalized with respect to the concentration of the dissolved polymer c_2 . Thus, it is a measure of how much the viscosity is affected by dissolving, e.g., 1 g of polymer.

$$\eta_{red} = \frac{\eta_{sp}}{c_2} \quad (3.144)$$

Because the reduced viscosity depends on the concentration of the dissolved polymer and is therefore influenced by deviation from ideal solution behavior, it is common practice to

2 One should not be tempted, however, to try to determine both M_n and M_w by using two calibration curves to interpret the numbers derived as the number and weight averages and finally even to determine a polydispersity index. The polydispersity obtained in this way would depend also on the polydispersity of the calibration substance. The errors involved make such an approach of little value.

extrapolate the measured values to zero concentration. The number so obtained is called the Staudinger index $[\eta]$:

$$\lim_{c_2 \rightarrow 0} \eta_{red} = [\eta] \quad (3.145)$$

The Staudinger index, also referred to as the intrinsic viscosity, does not vary with concentration as does the reduced viscosity. It is a measure of the volume of the polymer molecules in a dilute solution and has the same units as the reduced viscosity, mL/g (or dL/g).

In the theoretical description of this phenomenon we can view the polymer chains as impenetrable spheres. If we disperse such spheres in a liquid with a viscosity η_0 , the viscosity increases to a value η . The specific viscosity for small volume fractions φ_2 of the dispersed spheres can be described with the Einstein equation:

$$\eta_{sp} = \frac{\eta - \eta_0}{\eta_0} = 2.5 \cdot \varphi_2 \quad (3.146)$$

In a dilute solution the volume fraction ($V_1 + V_2 \approx V_1$), depends on the mass concentration c_2 , the mass of a single sphere m_2 and its volume v_2 as follows:

$$\varphi_2 = \frac{V_2}{V_1} = \frac{v_2}{m_2} c_2 \quad (3.147)$$

V_2	Volume of all spheres
V_1	Volume of the solvent
v_2	Volume of one sphere
m_2	Mass of one sphere

It is assumed that the polymer chains in the dilute solution are swollen with solvent, i.e., that the quotient $v_2 c$ is not simply the inverse of the density of the pure polymer but rather a larger value which depending on the quality of solvent.

By combining (3.146) and (3.147), one obtains

$$\frac{\eta - \eta_0}{\eta_0} \frac{1}{c_2} = 2.5 \cdot \frac{v_2}{m_2} \quad (3.148)$$

The term on the left hand side of (3.148) involves only experimentally measured values and is referred to as the reduced specific viscosity (see above). In practice, deviations are observed depending on the concentration of the solution. These can be eliminated by assuming an infinitely diluted solution ($c_2 = 0$, see Eq. 3.145) and use $[\eta]$ instead of the first term.

With (3.148), measuring the viscosity of a polymer solutions yields a measure for the quotient of the volume of a (swollen) polymer chain and its molar mass. For hard, solid spheres, e.g., highly cross-linked, sphere-shaped particles, $v_2 \sim m_2$. Thus, for such particles, the Staudinger index doesn't depend on the particle mass so that only information about the density of the particles but not their mass can be derived.

However, for solvent penetrated coils, Kuhn's square root law can be used whereby the average end-to-end distance, i.e., the effective diameter of the coil d_2 , is proportional to $\sqrt{m_2}$ (► Chap. 2).

Thus:

$$v_2 \sim d_2^3 \sim m_2^{3/2} \quad (3.149)$$

From (3.148) and (3.149) one obtains for the molar mass M_2 :

$$[\eta] \sim \frac{m_2^{3/2}}{m_2} \sim m_2^{1/2} \sim M_2^{1/2} \quad (3.150)$$

As a general case for the various structures of polymer molecules in solution, the so-called Mark–Houwink equation, (3.151), is used:

$$[\eta] = K_{M,H} \cdot M^a \quad (3.151)$$

$K_{M,H}$ Solution-dependent and polymer-specific constant

a Exponent, between 0.5 (ideal sphere) and 2.0 (stick-like molecules)

The preparation for viscometry measurements is comparatively simple. The time t is experimentally measured, for which a certain amount of a solution ΔV needs to flow through a capillary of a known diameter d . According to Hagen and Poiseuille's Law:

$$\eta = \frac{\pi \cdot g \cdot \Delta h \cdot d^4}{128 \cdot \Delta V \cdot l} \cdot \rho \cdot t \quad (3.152)$$

Here, g stands for the Earth's acceleration produced by gravity, Δh for the difference in height between the upper and lower reservoir of the liquid, l for the length of the capillary, and ρ for the density of the polymer solution. For a specific viscometer the quotient in (3.152) is constant so that a device constant K_G can be defined and (3.152) becomes

$$\eta = K_G \cdot \rho \cdot t \quad (3.153)$$

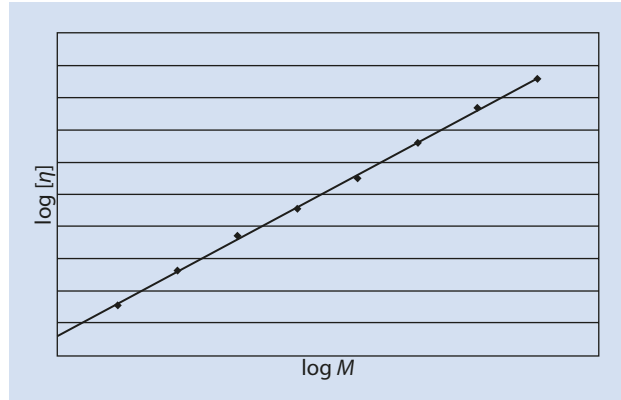
The device constant can be determined (if not supplied by the device manufacturer) using any pure solvent with a known viscosity and (3.154):

$$K_G = \frac{\eta_0}{\rho_0 \cdot t_0} \quad (3.154)$$

Here the variables indicated with 0 represent the density, viscosity, and time required by the pure solvent to flow through the capillary.

For dilute polymer solutions it can be assumed to a good approximation that the density of the polymer solution does not differ considerably from that of the pure solvent:

■ Fig. 3.17 Double logarithmic plot of the Staudinger index vs the molar mass



$$\rho \approx \rho_0 \quad (3.155)$$

so that

$$\eta = \eta_0 \cdot \frac{t}{t_0} \quad (3.156)$$

Thus, for a once calibrated apparatus the measurements are reduced to simply measuring the time for a certain amount of sample liquid. In modern viscometers this is done automatically. To reduce the error, multiple measurements are made. As the viscosity of polymer solutions is largely dependent on the temperature, excellent temperature control of the viscometer is extremely important to obtain reproducible results.

With the Mark–Houwink equation (3.151) a calibration with polymer probes of various molar mass, determined with other (absolute) methods, can be performed. The equation predicts that a double-logarithmic plot of the Staudinger index against the molar mass for different samples results in a straight line with gradient a and an intercept equal to the solvent and polymer dependent constant of the Mark–Houwink equation (■ Fig. 3.17).

From the value of the exponent a determined with this graph, important conclusions can be drawn about the shape of the dissolved polymer. An exponent of 0.5 indicates a solvent penetrated polymer in a θ -solvent (► Chap. 2). In thermodynamically better solvents, higher values of around 0.8 are observed. Even higher values of around 2 indicate that the polymer molecules are stiff or stick-shaped.

If the calibration—as explained in the introduction to ► Sect. 3.3—was made with monodisperse standards, the following average for the molar mass from the viscosity measurements is obtained; this is referred to as the viscosity average molar mass:

$$M_\eta = \left(\frac{\sum_i m_i M_i^a}{\sum_i m_i} \right)^{1/a} \quad (3.157)$$

At first glance, (3.157) looks rather complicated, but further consideration makes an interpretation relatively simple. For the number and the weight averages, the molar mass M_i is

averaged over the number or the weight of the fraction, respectively. By analogy, for the numerator in (3.157) for the viscosity average molar mass, the individual molar masses are averaged according to their contribution to the viscosity of the solution. According to (3.151), this is given by M^{ν} . This explains the exponent in the numerator of (3.157). The denominator is explained by the viscosity of a polymer solution being proportional to the total mass of the solute. Thus the viscosity average involves the mass of each molar mass fraction. The exponent for the quotient serves to arrive at a correct unit for the average molar mass. Also, if standards which are not strictly monodisperse are employed, a viscosity average molar mass is obtained, the value of which depends on how the calibration was performed.

A great advantage of the viscometry lies in the large range of molar mass which can be determined. For samples having extremely large or small molar mass, the flow rates can be varied by choosing a larger or smaller capillary. Even a molar mass >100 g/mol can be measured with a suitable solvent. The upper measurable molar mass limit is about $20 \cdot 10^6$ g/mol.

Because viscosity measurements to determine the Staudinger index require a concentration series ($c \leq 1$ g/100 mL) to be measured, ca. 250 mg of material is necessary.

As well as exceptionally good thermal control, it should also be noted that the method is extremely sensitive to dust particles and insoluble polymer. The solution should thus be filtered before the measurements and it should be confirmed that the polymer is completely soluble.

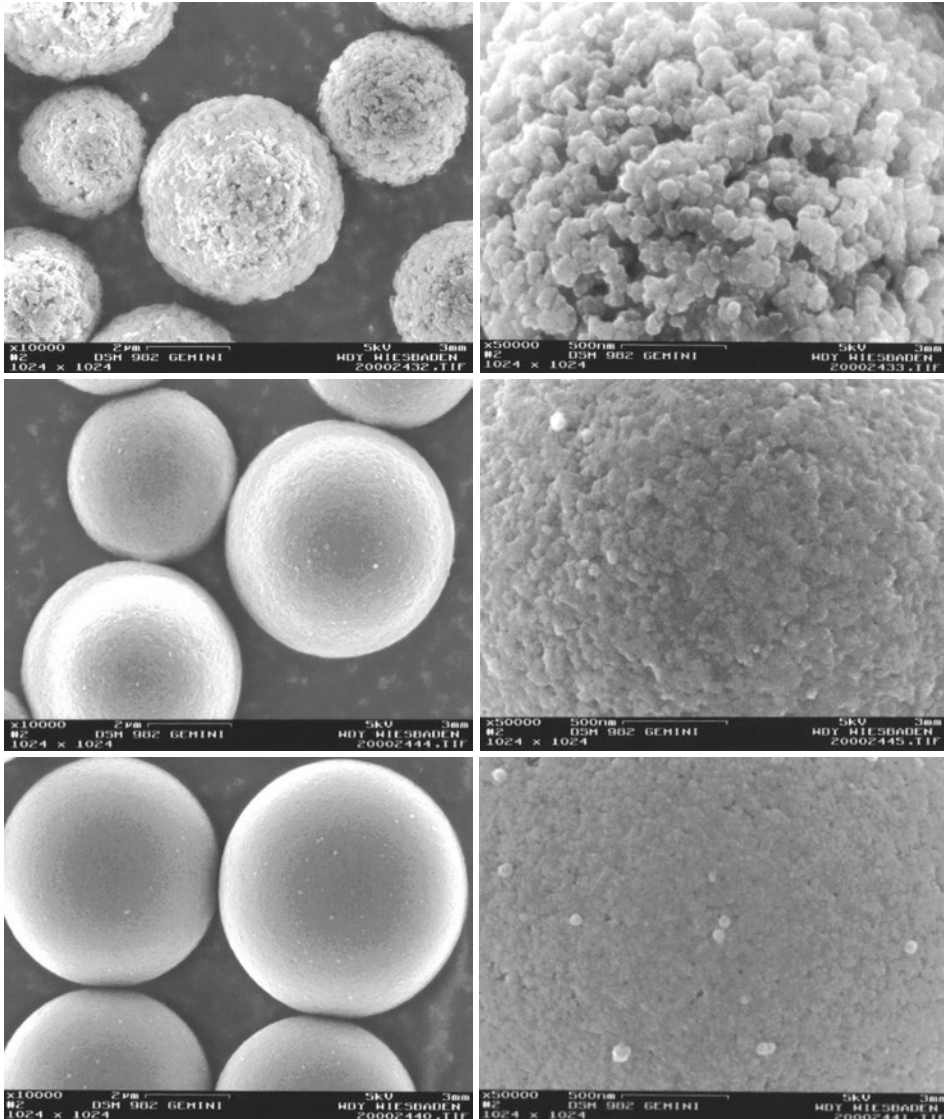
3.3.2 Size Exclusion Chromatography (SEC)

So-called *Size Exclusion Chromatography* is also referred to by the acronym SEC. In older literature, and the name *Gel Permeation Chromatography*, abbreviated as GPC, can also be found.

The apparatus preparation is, in principle, rather easy and similar to what is required for HPLC known from small molecule organic chemistry. The sample is introduced into the system with a syringe and carried by the mobile phase through one or more separation columns with the help of a pump. Detection at the exit of the column(s) is achieved by conventional methods, such as refractive index or UV/vis-detectors. However, in contrast to HPLC, the separation does not rely on a different adsorption of molecules to the stationary phase of the separation columns but rather on the different molecular size, more precisely; their different hydrodynamic radii. To achieve this, a porous polymer gel, i.e., a swollen, cross-linked polymer, is employed as the stationary phase. The size of the gel's pores is approximately equal to the size of the polymer molecules which can enter these pores. (■ Fig. 3.18) shows some electron micrographs of such a gel.

It is essential for the separation by size that the pores of the gel are of different sizes. As a result, a polymer of a certain molar mass (and thus of a certain size) can only enter into a certain proportion of these pores. The smaller the molecule, the larger the number of pores that it can enter during the chromatographic process. Thus, the smaller polymer molecules enter and exit a *larger* number of pores within the column and thus travel a longer distance when inside the column, and they exit the column *later* than larger molecules (■ Fig. 3.19).

The elution volume V_E at which the polymer of a certain molar mass exits the separation column, can be described by the following equation:

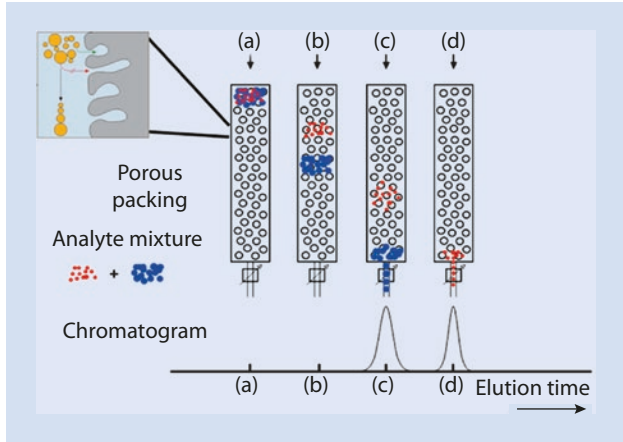


■ Fig. 3.18 Electron micrographs at various magnifications of SEC-gels with various pore sizes. (By kind permission of Polymer Standards Services GmbH, Mainz)

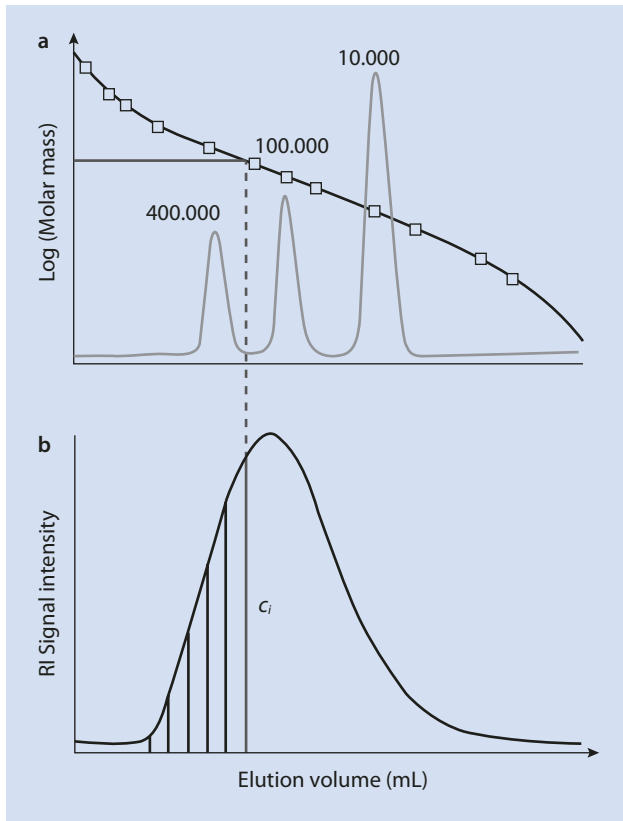
$$V_E = V_l + V_i \cdot f(M_2) \quad (3.158)$$

Here, V_l is the volume between the gel particles. V_i is the pore volume inside the gel particles. The course of the function denoted as $f(M_2)$ represents the fraction of the available pores that, because of their size, are able to accept macromolecules of molar mass M_2 . It has a value between 0 (very large molecules) and 1 (very small molecules). The form of the function defines the so-called upper and lower exclusion limit. Above a certain molar mass, the molecules are so large that they do not fit into any gel pores ($f(M_2)=0$). Above

■ **Fig. 3.19** Separation principle of SEC according to polymer size



■ **Fig. 3.20** (a) SEC calibration with standards having narrow molar mass distributions. (b) Determination of the concentration fractions c_i and the corresponding molar masses M_i of a polystyrene sample with a broad molar mass distribution. RI refractive index detector



this molar mass, no further separation occurs ($V_E = V_l$). All molecules leave the separation column at the same time at the minimum elution time. In analogy, a minimum molar mass also exists, below which the total pore volume of the stationary phase is available to the molecules ($f(M_2) = 1$). Thus for molecules smaller than the lower exclusion limit, no further

separation occurs ($V_E = V_I + V_i$). The molecules exit the column simultaneously at a maximum elution time. The function $f(M_2)$ and thus also the exclusion limits depend on the employed column as well as the eluent, the temperature, and the analyte. The calibration of the SEC is usually executed with standards of narrow molar mass distribution (often polystyrene) (■ Fig. 3.20).

The following equation is usually experimentally determined:

$$\log M = a - b \cdot V_E \quad (3.159)$$

Here a and b depend on the experimental setup and the column's stationary phase. Assigning a molar mass to an elution time (or an elution volume) is normally made simply from a calibration curve measured with standards having narrow molar mass distributions and of known molar mass (relative method). With such a calibration, a molar mass can be assigned to every elution volume. After recording the chromatogram it is normally analyzed by suitable software. With the assumption that the intensity of the detector signal corresponds to the concentration of the macromolecules, which is usually accurate enough, this analysis yields the number of molecules n_i for each molar mass M_i .

From this data set, all the average values can be calculated from the equations discussed at the beginning of this chapter. Furthermore, as well as this numerical information, a graphical representation of the molar mass distribution is directly available. This is especially important if the molar mass of the polymer being analyzed is not evenly distributed around a defined molar mass average but, instead, the molar mass distribution has multiple maxima. As opposed to the so-called *monomodal* samples in which the molar mass distribution has only a single maximum, such samples are referred to as *bimodal* or *polymodal*, depending on the number of maxima.

The separation of the macromolecules in SEC depends on their hydrodynamic volume V_h . This depends on the molar mass in a different way for each polymer. To avoid needing to consider dependence of the physical chemical properties on the particular polymer, the following equation (without proof) can be employed:

$$\log(M \cdot [\eta]) \propto V_h \quad (3.160)$$

Thus, the hydrodynamic volume of a polymer should be independent of its chemical composition and its microstructure, so that for a given chromatography column and a certain solvent it should be proportional to the logarithm of the product of the Staudinger index and the molar mass. Indeed, this can be confirmed by experiment and a plot of the logarithm of this product vs the elution volume results in a straight line to a good approximation (■ Fig. 3.21). (Grubisic et al. 1967; Wild and Guliana 1967).

A great advantage of SEC is the speed and simple execution of the measurement. Only ca. 0.1 mg is injected onto the column as a dilute solution. The measurement of different concentrations is unnecessary. The range of molar mass which can be measured depends on the exclusion limits of the separation column. As opposed to most of the methods presented in this chapter, the SEC delivers any desired molar mass average and offers information about the shape of the molar mass distribution. These advantages have led to great importance being placed on the molar mass definition with SEC in practice. However, two key limiting conditions must be kept in mind when using this method:

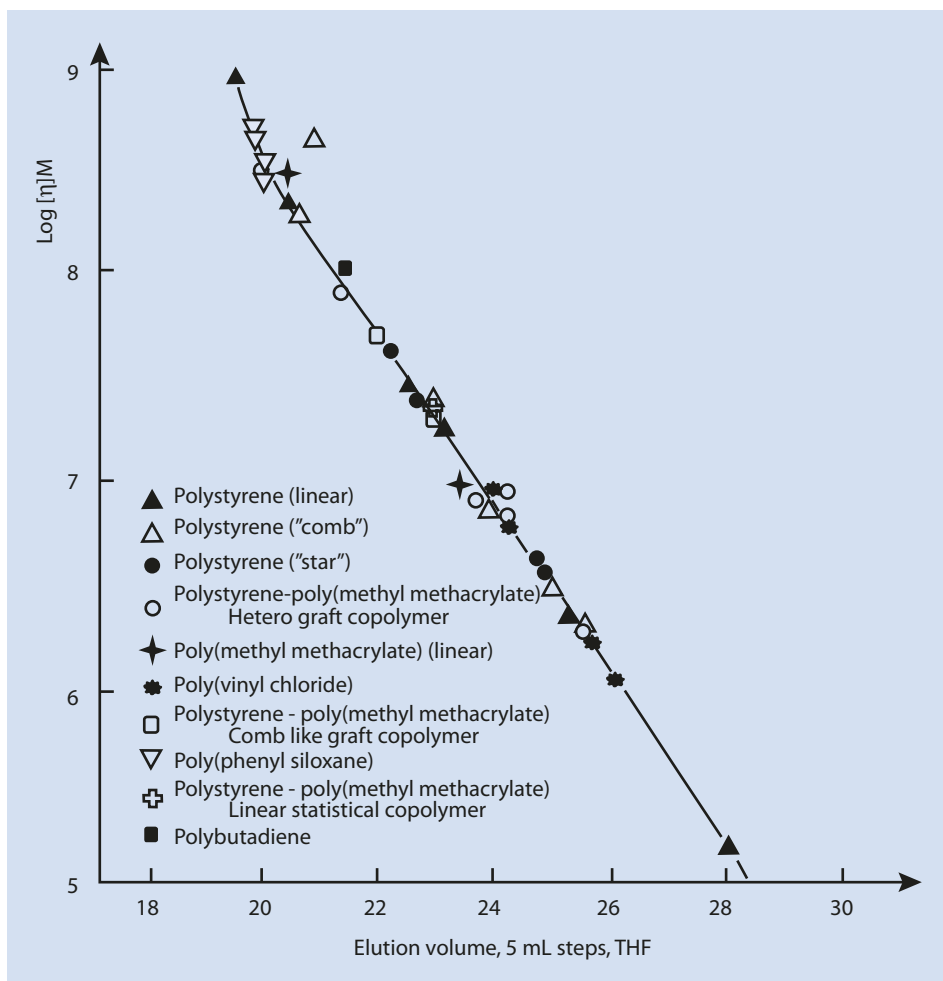


Fig. 3.21 Example of a universal calibration with THF as solvent

1. The interactions between polymer, solvent and column packing should be approximately equal for all combinations, and preferably as minimal as possible. If the polymer interacts with the stationary phase, for example, the separation according to hydrodynamic volume is superimposed by effects common to adsorption chromatography. Choosing a suitable column that meets all the criteria in the best possible way is therefore crucial for meaningful results.
2. Because of the inherent influence of the solvent quality on the effective size of the polymer (see above), the system of calibration standard and solvent has a great influence on the determined molar mass of the measured sample, especially if the polymers being examined differ chemically from the standard. Thus, it is essential to report the standard used. Because this is often polystyrene, the determined molar mass should be given as a polystyrene equivalent molar mass (in the solvent used).

3. In some co-polymerization processes it can happen that some comonomers are preferentially incorporated in polymer molecules having greater or smaller molar mass so that the chemical composition of the polymer is not the same over the molar mass distribution. Such chemical inhomogeneity with respect to the molar mass can indeed make the quantitative evaluation of the detector questionable. In such cases, multidimensional chromatography techniques that combine the SEC with conventional chromatography techniques can provide a solution (Rittig and Pasch 2008).

The combination of static light scattering and SEC and a concentration-dependent detector (RI- or UV/vis) yields absolute molar mass information without the necessity of a calibration and thus provides more information about the sample, simultaneously retaining the advantages of SEC.

The speed and simplicity of SEC and viscometry have made these methods standard practice in industrial polymerization processes where they are routinely employed to verify adherence to product specification where molar mass is involved.

Both SEC and viscometry are relative methods. If an absolute molar mass is required, a characterization by light scattering (if necessary, coupled with SEC) or analytical ultracentrifugation is recommended. These methods are also convenient if no appropriate, inert column material can be found.

For the characterization of comparatively small macromolecules, MALDI-TOF or osmometry can be successfully employed.

References

- Grubisic Z, Rempp P, Benoit H (1967) A universal calibration for gel permeation chromatography. *Polym Lett* 5:753–759
- Maechtle W, Boerger L (2006) *Analytical ultracentrifugation of polymers and nanoparticles*. Springer, Heidelberg
- Meselson M, Stahl FW (1958) The replication of DNA in *Escherichia coli*. *Proc Natl Acad Sci* 44:671–682
- Pasch H, Schrepp W (2003) MALDI-TOF mass spectrometry of synthetic polymers. Springer, Heidelberg
- Rittig F, Pasch H (2008) Multidimensional liquid chromatography in industrial applications. In: Cohen SA, Schure MR (eds) *Multidimensional liquid chromatography, theory and applications in industrial chemistry and the life sciences*. Wiley, New York, pp 387–423
- Schaertl W (2007) *Light scattering from polymer solutions and nanoparticle dispersions*. Springer, Heidelberg
- Svedberg T, Pedersen KO (1940) *The ultracentrifuge*. Oxford University Press, Oxford
- Wild L, Guliana R (1967) Gel permeation chromatography of polyethylene: effect of long chain branching. *J Polym Sci A-2*(6):1087–1101